Galileo Telecommunications

Jim Taylor, Kar-Ming Cheung, and Dongae Seo

July 2002

JPL DESCANSO

Deep Space Communications and Navigation Systems Center of Excellence

Design and Performance Summary Series

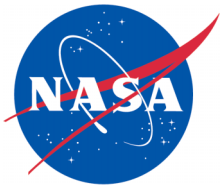

DESCANSO Design and Performance Summary Series

Article 5

Galileo Telecommunications

Jim Taylor
Kar-Ming Cheung
Jet Propulsion Laboratory
California Institute of Technology
Pasadena, California

Dongae Seo
International Space University
Strasbourg, France

National Aeronautics and Space Administration

Jet Propulsion Laboratory
California Institute of Technology
Pasadena, California

July 2002

This research was carried out at the
Jet Propulsion Laboratory, California Institute of Technology,
under a contract with the
National Aeronautics and Space Administration.

Galileo: Orbiter and Probe Mission to Jupiter

The cover image shows the Galileo orbiter, as it communicates with the Earth, superimposed against Jupiter with the large Jovian satellites Io, Europa, Ganymede, and Callisto (top to bottom) at the right.

Galileo has accomplished a remarkable mission despite the orbiter's downlink data rate being much lower than originally planned because, as the picture shows, the high-gain antenna failed to deploy fully. After the orbiter had collected data as it flew past Venus in 1990 and Earth in both 1990 and 1992, the orbiter and the attached probe continued toward Jupiter even while a wholly new "S-band mission," described in this article, was being planned to accommodate the availability of only a low-gain antenna. The new mission required creative adaptation in the flight software to enable data compression, packet telemetry, and improved error-correction coding. At the same time, the ground receiving system was upgraded to provide for real-time intercontinental arraying of ground antennas and a feedback concatenated decoding scheme. On the way to Jupiter, the orbiter collected data at two asteroids, including the satellite of one, and from the impacts into Jupiter of a fragmented comet.

The images that introduce the Preface are of the orbiter (left) and the probe (right) as they arrived at Jupiter on December 7, 1995.

The probe entered Jupiter's atmosphere at 170,000 km/hr, slowed and descended 150 km through the top layers of the atmosphere, transmitting science data for a little more than one hour before increasing temperature and pressure destroyed it. The orbiter received the probe data via a relay link, artistically denoted by the blue dots. Within an hour after the probe data ended, the orbiter fired its main engine to brake into orbit around Jupiter. The orbiter sent the data to the Deep Space Network on Earth via its low-gain antenna. It then began its planned prime science mission of collecting fields and particles data, radio science, and images during ten satellite flyby encounters. Two years later, the Galileo Europa Mission began. Most recently, the orbiter has been working through the Galileo Millennium Mission, with a close flyby of the satellite Amalthea planned in late 2002 and a mission-completion plunge into Jupiter's atmosphere in 2003. Through May 2002, the orbiter has completed 33 orbits around Jupiter, including repeated flybys of the four major Jovian satellites shown on the cover.

This article was originally published on the website, *DESCANSO: Deep Space Communications and Navigation Systems*, http://descanso.jpl.nasa.gov/index_ext.html

DESCANSO DESIGN AND PERFORMANCE SUMMARY SERIES

Issued by the Deep-Space Communications and Navigation Systems
Center of Excellence
Jet Propulsion Laboratory
California Institute of Technology

Joseph H. Yuen, Editor-in-Chief

Previously Published Articles in This Series

Article 1—"Mars Global Surveyor Telecommunications"
Jim Taylor, Kar-Ming Cheung, and Chao-Jen Wong

Article 2—"Deep Space 1 Telecommunications"
Jim Taylor, Michela Muñoz Fernández, Ana I. Bolea Alamañac, and Kar-Ming Cheung

Article 3—"Cassini Telecommunications"
Jim Taylor, Laura Sakamoto, and Chao-Jen Wong

Article 4—"Voyager Telecommunications"
Roger Ludwig and Jim Taylor

Table of Contents

List of Figures

List of Tables

Foreword

This Design and Performance Summary Series, issued by the Deep Space Communications and Navigation Systems Center of Excellence (DESCANSO), is a companion series to the DESCANSO Monograph Series. Authored by experienced scientists and engineers who participated in and contributed to deep-space missions, each article in this series summarizes the design and performance for major systems such as communications and navigation, for each mission. In addition, the series illustrates the progression of system design from mission to mission. Lastly, it collectively provides readers with a broad overview of the mission systems described.

Joseph H. Yuen
DESCANSO Leader

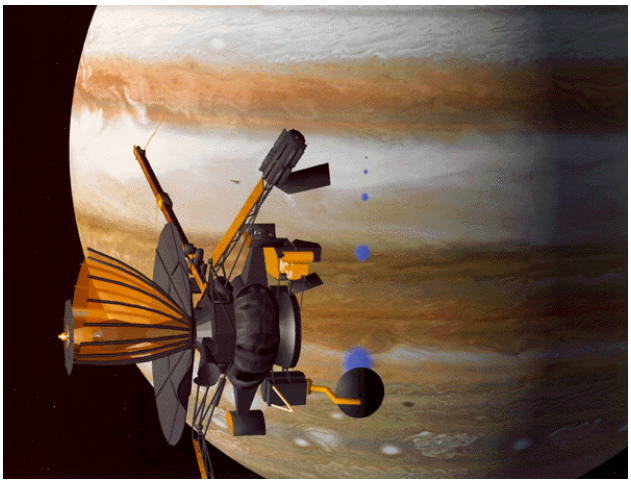

Preface

This article describes how the Galileo orbiter and the Deep Space Network (DSN*) ground systems receive and transmit data. The relay communications subsystems and the link between the Galileo probe and the orbiter are also described briefly. The article is at a functional level, intended to illuminate the unique mission requirements and constraints that led to both design of the communications system and how it has been modified and operated in flight.

The primary purpose of this article is to provide a reasonably complete single source from which to look up specifics of the Galileo radio communications. Augmenting the spacecraft downlink design and the supporting ground system for science return with only the low-gain antenna was a particular challenge for the Galileo planetary mission, as detailed in Section 4. This article will be updated when needed as the Galileo Millennium Mission (GMM) progresses.

The Galileo orbiter was designed and built at the Jet Propulsion Laboratory (JPL) in Pasadena, California, and the Galileo probe at the NASA Ames Research Center in Sunnyvale, California. The orbiter flight team is located at JPL, as was the probe flight team during that portion of the mission.

Much of the Telecom design information in this article was obtained from original Galileo prime mission design documentation: the design control document for the telecommunications links [1] and the functional requirements for the orbiter's Telecommunications System and the hardware subsystems [2]. Much of the mission and operational information came from the Galileo public website, Shannon McConnell, website curator [3].

* Look up this and other abbreviations and acronyms in the list that begins on page 63.

Acknowledgements

The authors would like to express their appreciation to many individuals in the Interplanetary Network Directorate (IND) and the Telecommunications Science and Engineering Division (33) at JPL for their encouragement and support during the preparation of this article. The authors are especially grateful to Pat Beyer, Tiffany Hue Chiu, Roger Ludwig, Eilene Theilig, and Steve Townes for their advice, suggestions, and helpful information.

Section 1

Mission and Spacecraft Description

1.1 The Mission

The Galileo spacecraft was launched in 1989 aboard the Space Shuttle Atlantis (STS* [Space Transportation System]-34). Its primary objective has been to study the Jovian System. The Galileo launch delay after the Challenger Space Shuttle accident in 1986 necessitated a change in the strategy to get Galileo to Jupiter.[1] The new mission plan made use of gravitational assists from Venus once and Earth twice to give the spacecraft enough energy to get to Jupiter. During the cruise phase of the mission,[2] the Galileo spacecraft took the first close-up images of an asteroid (Gaspra) in October 1991, and discovered the first known moon (Dactyl) of an asteroid (Ida) in August 1993. During the latter part of the cruise, Galileo was used to observe the collisions of fragments of Comet Shoemaker-Levy 9 with Jupiter in July 1994.

The Galileo primary mission (1995–1997) involved

- Penetration of Jupiter's atmosphere by the probe that returned a Jovian "weather report" on temperature, pressure, composition, winds, clouds, and lightning
- Initial orbiter flyby of the Jovian satellite Io and passage through the Io torus
- Jupiter orbit insertion (JOI)
- A two-year "tour" of the major satellites by the orbiter that returned images, radio science, and data on fields and particles.

The probe descended through an unusually dry spot in Jupiter's top cloudy layer, and probably melted in the hot atmosphere somewhere below the clouds.

The orbiter has six scientific instruments on one section that spins (3 rpm), for pointing stability and for collecting three-dimensional fields and particles data near the spacecraft. The

---

* Look up this and other abbreviations and acronyms in the list that begins on page 63.

[1] The last planetary launch before Galileo in 1989 was Pioneer Venus in 1978. Galileo remained in "new mission" status for these years while the launch vehicle was changed four times. Each change, none of them due to the Galileo spacecraft itself, necessitated a complete redesign of the mission with corresponding changes to the requirements for tracking and data acquisition support by the DSN [4].

[2] Refer to http://www.jpl.nasa.gov/missions/current/galileo.html for more on the interplanetary mission design.

"de-spun" section uses gyros to point the four remote-sensing instruments at a target to obtain images, composition, surface structure, and temperature data.[3] The orbiter's umbrella-like high-gain antenna did not deploy, so Galileo's computer was reprogrammed to compress and record the data taken during Jovian satellite flybys to the on-board tape recorder. The data is returned to Earth during the remainder of each orbit using the low-gain antenna and modifications to the ground receiving systems of the Deep Space Network. The orbiter is powered by two radioisotope-thermoelectric-generators (RTGs). It used its 400-N main engine to go into Jupiter orbit, but maintains pointing and fine-tunes each new orbit with clusters of 10-N thrusters.

The prime-mission tour consisted of 11 different elliptical orbits around Jupiter, with each orbit (except one) involving a close flyby and gravity assist at Jupiter's moons Ganymede, Callisto, or Europa. The major scientific returns from the primary mission included data on

- Jupiter's storms and rings
- Hot, active volcanoes on Io
- A possible ocean on Europa
- Ganymede's own magnetic field
- The possibility of an ocean beneath Callisto's surface.

Galileo discovered strong evidence that Europa has a liquid saltwater ocean under an ice layer on its surface. The spacecraft also found indications that two other moons, Ganymede and Callisto, have layers of liquid saltwater as well.

After completing its primary mission, Galileo began a two-year extended mission called the Galileo Europa Mission (GEM) on December 8, 1997. GEM was a 14-orbit, low-cost extension of Galileo's exploration of the Jovian system. This mission was divided into three main phases: (a) the Europa Campaign (December 1997–May 1999) which searched for further signs of a past or present ocean beneath Europa's icy surface, (b) the Jupiter Water/Io Torus Study (May 1999–October 1999) which focused on detailed storm and wind patterns in Jupiter's atmosphere, and (c) the Io Campaign (October 1999–December 1999) which obtained, from two flybys, high-resolution images and a compositional map of Io with a sample of a volcanic plume.

At the end of the GEM, December 31, 1999, the orbiter started another mission called the Galileo Millennium Mission (GMM). This mission originally was planned for completion within approximately 14 months but has been extended to 2003. The GMM mission plan originally consisted of two phases, first Io and then Cassini.[4] It now also includes plans for the final disposition of the orbiter.[5] During the GMM, the orbiter made additional close flybys of all four large moons, including four encounters of Io from 2000 through 2002. The spacecraft has studied I's extensive volcanic activity and the magnetic environment at high resolution. It also observed Europa's ionosphere, generated by ultraviolet radiation from the Sun and interaction of the charged particles from the Jovian magnetosphere. In the Cassini phase, the spacecraft performed cooperative measurements with the Cassini spacecraft as Cassini received its own gravity assist from Jupiter in December 2000. Galileo was also relatively near Jupiter at that time. Galileo collected data from Jupiter's inner magnetosphere, the dusk side of the magnetosphere and the solar wind.

---

[3] The last remote sensing data from the orbiter was received in March 2002. See Epilogue of this article.

[4] Refer to http://www.jpl.nasa.gov/jupiterflyby/ and http://galileo.jpl.nasa.gov/news/release/press020227.html for more on the Galileo/Cassini 2001-2002 cooperative mission.

[5] Refer to http://www.jpl.nasa.gov/news/fact_sheets/galileo.pdf for more information on the current GMM and a table showing the dates and flyby altitudes of all of Galileo's satellite encounters.

In November 2002, Galileo will swing closer to Jupiter than ever before, flying less than 1000 km over the moon Amalthea,[6] which is less than one-tenth the size of Io and less than half as far from Jupiter. Measurements of changes in Galileo's radio signal frequencies during the flyby will be used refine the mass and density of Amalthea. This passage will also produce information on dust particles as Galileo flies through Jupiter's gossamer rings as well as new information on magnetic forces and energetic charged particles close to the planet. Galileo's final orbit will take an elongated loop away from Jupiter. Then in September 2003, comes a mission-ending plunge into Jupiter's atmosphere to ensure against the possibility of impact and Earthly contamination of any Jovian satellites. Eight years after probe entry, the orbiter will also make a direct impact with Jupiter, vaporizing as it plows into the dense atmosphere.

1.2 The Spacecraft

The Galileo spacecraft (Fig. 1-1) had two main components at launch, the 6.2-m tall orbiter, and the 0.9-meter long probe.[7] The orbiter's launch mass was 2,223 kg, including a 118-kg science payload and 925 kg of usable propellent.[8] The probe's total mass was 339 kg: the probe descent module was 121 kg, including a 30-kg science payload.

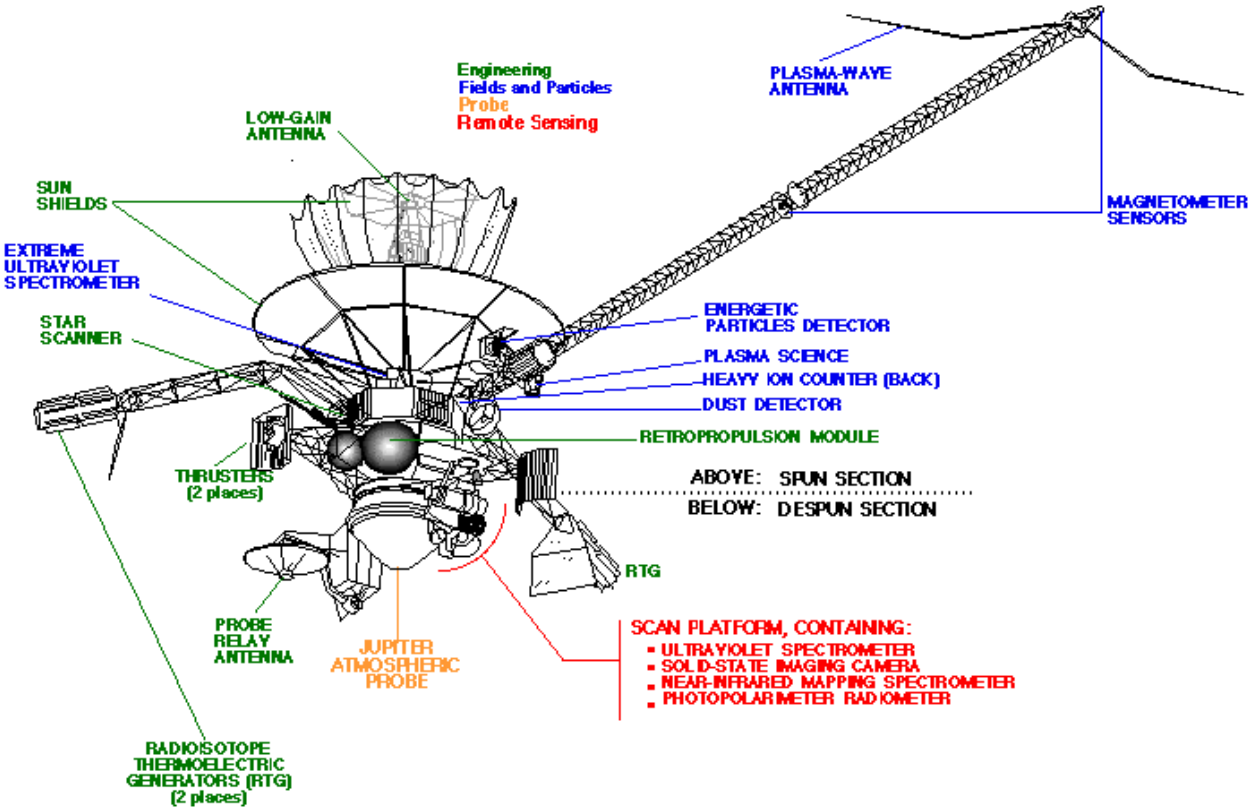

Fig. 1-1. Galileo spacecraft.

[6] Amalthea averages 189 km in diameter (270 × 166 × 150). Amalthea was the nymph who nursed the infant Jupiter with goat's milk. http://seds.lpl.arizona.edu/nineplanets/nineplanets/nineplanets.html

[7] The spacecraft description and Figs. 1-1 and 1-2 come from http://www.jpl.nasa.gov/galileo/tour/4TOUR.pdf. This document contains descriptions of the spacecraft subsystems and science instruments.

[8] Propellant made up 41% of the orbiter's launch mass. Most of the propellant was consumed at JOI.

1.2.1 Galileo Orbiter

The Galileo orbiter combines features of spinner spacecraft (the Pioneers and Ulysses) and three-axis-stabilized spacecraft (the Voyagers). The orbiter incorporates an innovative "dual-spin" design. Part of the orbiter (including the telecom electronics and antennas and some instrument booms) rotates while another part (containing an instrument platform) remains fixed in inertial space. The orbiter is a good platform for fields and particles experiments that perform best when rapidly gathering data from different directions. The orbiter is also a good platform for remote sensing experiments that require accurate and steady pointing.

The orbiter uses two RTGs to supply electrical power to run the spacecraft's devices. The radioactive decay of plutonium produces heat that is converted to electricity. The RTGs produced about 570 W at launch. The power output decreases at the rate of 0.6 W per month and was 493 W when Galileo arrived at Jupiter.

The attitude and articulation control subsystem (AACS) is responsible for determining the orientation of the spacecraft in inertial space, keeping track of the spacecraft orientation between attitude determinations, and changing the orientation, instrument pointing, spin rate, or wobble of the spacecraft. Software in the AACS computer carries out the calculations necessary to do these functions. As part of the S-band mission (Section 4 of this article), the AACS software was updated to include the ability to compress imaging and plasma wave data down to as little as 1/80th of their original volume.

There are 12 scientific experiments aboard the Galileo orbiter. The despun section is home to four remote-sensing instruments (labeled in red in Fig. 1-1), mounted on the scan platform with their optical axes aligned so that they view a nearly common area. The spun section contains six instruments (labeled in blue) that investigate particles and magnetic fields. Two radio-science investigations (celestial mechanics and radio propagation) do not have individual instruments but piggyback on the orbiter's telecom system, including an ultrastable oscillator.

Figure 1-2 shows the wavelength ranges of the electromagnetic spectrum that the remote-sensing instruments have monitored during both encounters and cruise periods.

1.2.2 Galileo Probe

The probe consisted of two main parts, the deceleration module and the descent module.[9] The deceleration module was required for the transition from the vacuum and cold of interplanetary space to the intense heat and structural loads incurred during a hypersonic entry into a planetary atmosphere—and from a speed of tens of kilometers per second to a relatively placid descent by parachute. The descent module carried the scientific instruments and supporting engineering subsystems that collected and transmitted scientific data to the orbiter that was flying overhead.

The probe did not have an engine or thrusters so it could not change the path set for it by the orbiter at separation. The probe was spin-stabilized, achieved by spinning the orbiter up to 10.5 rpm before release. There was no communication between orbiter and probe during the coast to Jupiter because the probe had no capability to receive radio signals. During atmospheric entry, the probe stored no data, collecting and transmitting it in real time.

---

[9] The probe description comes from http://www.jpl.nasa.gov/galileo/tour/5TOUR.pdf. See Section 7 of this article for more detail on the probe-to-orbiter relay link.

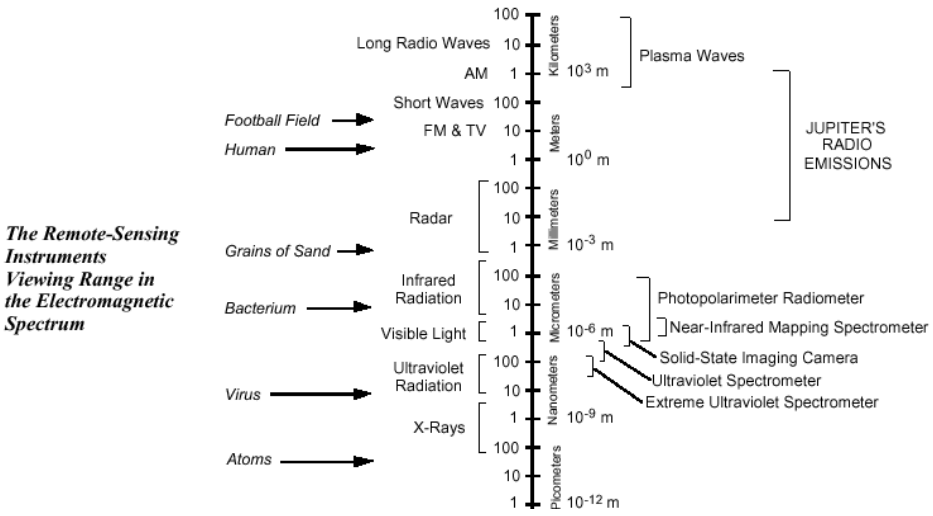

Fig. 1-2. Orbiter's remote sensing instrument wavelength ranges.

The probe's entry into the Jovian atmosphere generated temperatures of 14,000 K. The materials used for the probe's descent module heat shields—carbon phenolic for the forebody shield and phenolic nylon for the afterbody shield—have also been used for Earth re-entry vehicles.

Parachutes were used for two key functions, separating the deceleration and descent modules and providing an appropriate rate of descent through the atmosphere. Before deployment of the main chute, a smaller, pilot parachute was fired at 30 m/s by a mortar to start the deployment process. The deployment occurred in less than 2 s, pulling away the aft cover and unfurling the main chute. The main parachute's diameter was 2.5 m. The canopy and lines were made of Dacron and Kevlar, respectively. Once the main chute was fully deployed, the forebody shield (aeroshell) was jettisoned.

To save weight, the Galileo descent module, carrying six scientific instruments, was not sealed against the influx of the Jovian atmosphere. However, the two relay radio systems were hermetically sealed within housings designed to withstand pressures up to 20 bars and tested to 16 bars.

Section 2

Galileo Spacecraft Telecommunications System

The telecom system is on the spun section of the dual-spin orbiter. The system consists of four hardware subsystems:

- Radio frequency subsystem (RFS)*
- Modulation demodulation subsystem (MDS)
- S-/X-band[1] antenna (SXA) subsystem
- X- to S-band downconverter (XSDC).

2.1 Galileo Telecommunications Functions and Modes

The Galileo telecommunications system[2] enables the orbiter to provide: (a) uplink carrier tracking and downlink carrier generation, (b) command detection, (c) telemetry encoding and modulation, and (d) radiometric communications with the Deep Space Network (DSN).[3] For interplanetary cruise, Galileo originally planned to use a ground station operated by the German Space Operations Center (GSOC)[4] as well as those of the DSN. During the prime mission, antenna arrays included the Parkes antenna operated by the Australian Commonwealth Scientific and Industrial Research Organization (CSIRO).[5]

---

* Look up this and other abbreviations and acronyms in the list that begins on page 63.

[1] For Galileo, S-band refers to carrier frequencies of about 2.1 GHz (uplink) and 2.3 GHz (downlink). X-band refers to carrier frequencies of about 7.2 GHz (uplink) and 8.4 GHz (downlink).

[2] Sections 2 and 3 describe the Galileo orbiter telecom system and the ground system as they were originally intended for use. References to uplink or downlink at X-band assume the availability of a fully deployed high-gain antenna (HGA). As described in Section 4, the HGA did not deploy. The X-band parts of the RFS were verified operational in short tests in 1991 and 1993. The S-band parts of the telecom system that use the LGA have functioned as designed.

[3] The terms “radiometric communications” or radiometric data in this article refer collectively to one-way or two-way Doppler, turnaround (sequential) ranging, and differential one-way ranging (DOR).

[4] Current information about GSOC is available at http://www.weblab.dlr.de/rbweb/index_e.asp

[5] Current information about the Parkes antenna is available at http://wwwatnf.atnf.csiro.au/

2.1.1 Uplink

Depending on the required uplink mode, the carrier may be unmodulated, modulated with a command subcarrier or ranging modulation, or both.

2.1.1.1 Uplink Carrier. The spacecraft receiver can acquire an uplink carrier arriving close enough in frequency, and then maintain phase-lock on that carrier as long as it is present. The telecom system is able to operate in the following uplink modes:

- With an uplink or with no uplink
- With the uplink at S-band or at X-band
- With the uplink modulated or unmodulated
- With the uplink transmitted from the either the DSN or GSOC.

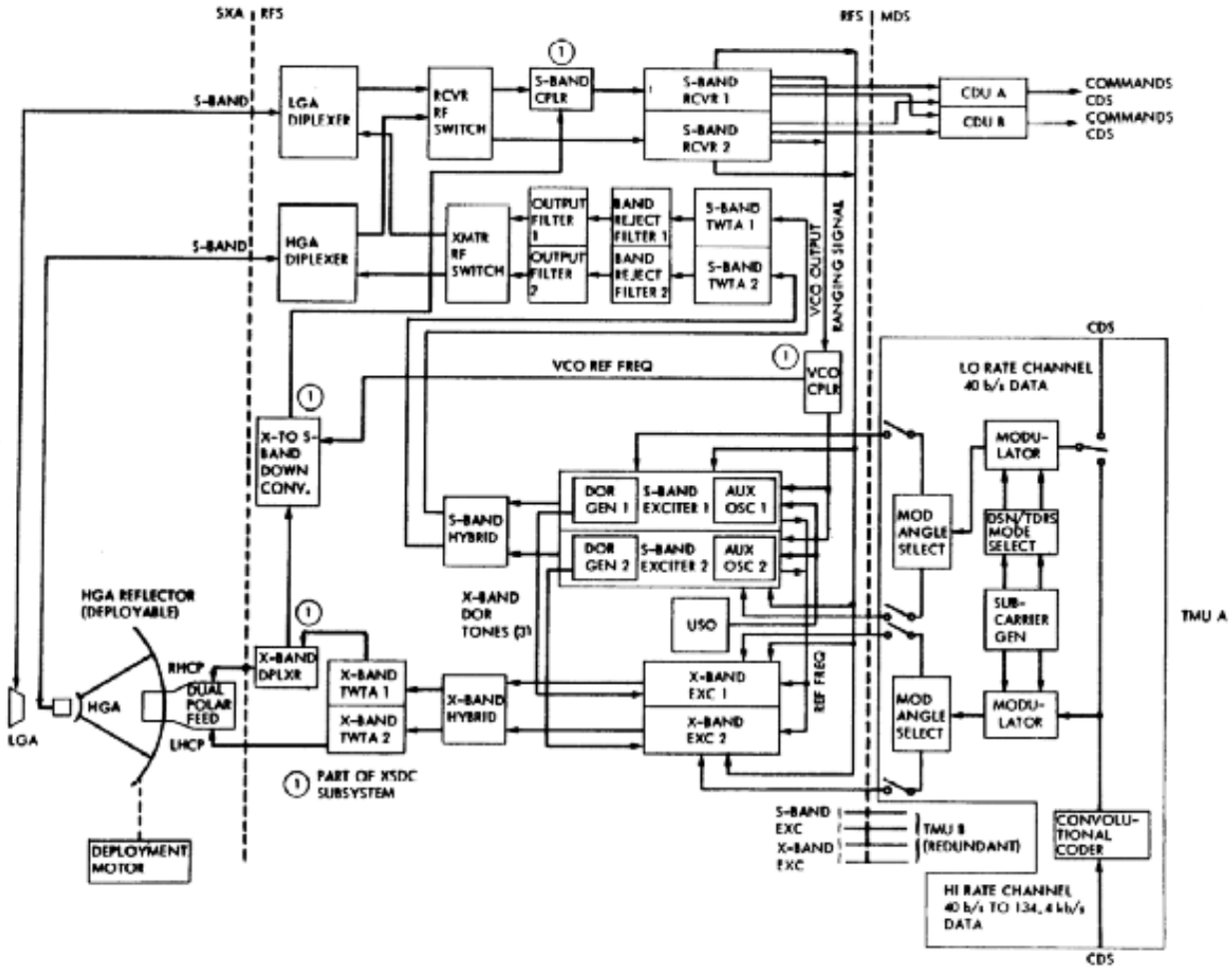

Fig. 2-1. Galileo orbiter telecom system.

2.1.1.2 Command Detection. The RFS S-band receiver (S-RCVR) and the command detector unit (CDU) receive and demodulate the command waveform from either an S-band or an X-band uplink carrier, and send it to the hardware command decoder in the command data subsystem

(CDS). The command waveform may be present alone or simultaneously with ranging modulation.

2.1.2 Downlink

The downlink carrier may be unmodulated, modulated with a telemetry subcarrier or ranging modulation or both.

2.1.2.1 Downlink Carrier. The RFS exciters (EXC) and power amplifiers make up the transmitters that give the orbiter the capability to generate, modulate, and transmit downlink carriers. With or without an uplink carrier present, the RFS is able to generate and transmit an S-band downlink carrier alone, an X-band downlink carrier alone, or both simultaneously. With either an S-band or X-band uplink carrier present, the RFS has the capability to use the uplink carrier to generate downlink S-band or X-band carrier frequencies or both. The S-band and X-band downlink carriers are always coherent with each other. Depending on RFS mode, the downlink carriers both are coherent with the uplink carrier or both are noncoherent.[6]

2.1.2.2 Telemetry Encoding and Modulation. The MDS's telemetry modulation unit (TMU) and the RFS's S-band exciter (S-EXC) and X-band exciter (X-EXC) process the telemetry "low-rate" and "high-rate" data-bit streams[7] from the CDS into modulated telemetry subcarriers that phase modulate the downlink carriers. The TMU provides two telemetry modes: Tracking and Data Relay Satellite System (TDRSS)[8] and DSN.

2.1.3 Radiometric Data

Radiometric communications are those that are required of the telecom system to meet project navigation and radio science data quantity and accuracy requirements. Radiometric data used with Galileo includes two-way or one-way Doppler, turnaround ranging, and differential one-way ranging (DOR).

2.1.4 Probe Relay

The L-band[9] relay link from the probe to the orbiter, active for about one hour on December 7, 1995, used equipment entirely separate from the orbiter's S-band and X-band uplink and downlink. **Section 7** describes the relay link and its telecom-related results in more detail.

The orbiter-mounted relay receiving hardware (RRH) received the L-band signal from the probe. Though mounted on and in the orbiter, the RRH antenna and receivers were designated part of the probe system. To eliminate single-point, catastrophic mission failures, the relay link

---

[6] Galileo is one of many JPL deep-space missions that have two downlink modes called "TWNC on" and "TWNC off." TWNC (two-way non-coherent) is pronounced "twink." The TWNC-on mode means the downlink frequency cannot be coherent with an uplink frequency. The TWNC-off mode means the downlink will be coherent with a received uplink when the transponder's receiver is in lock to the uplink carrier.

[7] As more fully described in Section 2.3, the CDS continuously outputs to the TMU both a 40 bps low-rate data stream and a high-rate data stream. The bit rate of the high-rate stream is set between 10 bps and 134.4 kbps, so in most cases its bit rate is higher than the fixed 40 bps of the low-rate channel.

[8] In the TDRSS mode, the TMU convolutionally coded a 1200-bps data stream received from the CDS. The symbol stream phase-modulated the RFS S-band RF carrier at 90±3 deg, without use of a telemetry subcarrier. This mode was used only for the immediate post-launch phase while the spacecraft was still attached to the Inertial Upper Stage (IUS). See **Operational Scenarios**.

[9] L-band refers to frequencies between 390 MHz and 1550 MHz. The probe-to-orbiter relay link carriers were 1387.0 MHz and 1387.1 MHz, chosen to provide the best link performance through Jupiter's atmosphere.

system configuration included two nearly identical RF links with dual electrical and electronic probe transmitting and orbiter receiving systems. Two parallel and simultaneous data streams went from the probe's scientific instruments to the orbiter. One of the data streams used an ultrastable oscillator for transmission to the orbiter. The probe Doppler wind experiment used variations in the frequencies of the carrier signals received at the orbiter to deduce the wind speeds in the atmosphere [5].

2.2 Radio Frequency Subsystem

The RFS has the major components listed in Table 2-1. The table includes the subsystem acronyms for reference.

Table 2-1. RFS components.

Element	Number of Units
S-band receiver (S-RCVR)	2
S-band exciter (S-EXC)	2
X-band exciter (X-EXC)	2
Ultrastable oscillator (USO)	1
S-band traveling-wave-tube amplifier (S-TWTA)	2
X-band traveling-wave-tube amplifier (X-TWTA)	2
Differential one-way ranging (DOR) generator	1
S-band antenna switches (LGA-1/LGA-2 switches, HGA/LGA switch)	2,1
Microwave routing and interface elements	N/A

Where there are duplicated units in a pair (such as S-RCVRs), generally each can provide full functionality. The units are cross-strapped but with only one unit powered at a time.[10] For example, either S-RCVR can drive either S-EXC, with the powered receiver driving the powered exciter. Similarly, either S-EXC can drive either S-TWTA. Additional functional redundancy was built into the RFS in the sense that the 1-way downlink frequency source can be either the exciter's auxiliary oscillator or the USO, and (when using the high-gain antenna [HGA]), the downlink could be at either S-band or X-band.

2.3 Modulation Demodulation Subsystem

The MDS consists of two TMUs and two CDUs, with one CDU and one TMU powered at a time. The CDU is responsible for the detection (demodulation) of uplink command data for decoding by the CDS, and the TMU is responsible for the modulation of telemetry data for downlink transmission.

Because of the critical functions performed by the CDU and TMU, each has a large amount of hardware redundancy and cross-strapping with the interfacing RFS elements. The two CDUs

[10] The term "cross-strapped" refers to the interconnections at the unit input or output. Because RCVR-1 and RCVR-2 are cross-strapped with S-EXC-1 and S-EXC-2, the transponder can operate with RCVR-1 driving either S-EXC-1 or S-EXC-2, or RCVR-2 driving either S-EXC. "Generally" means there are exceptions, required either in hardware design or flight rule, or a factor in selecting configuration [2]. RFS exceptions to "generally": Only RCVR-1 is connected to the XSDC. RCVR-2 operates on the same channel as the USO, so potential frequency interference was one factor in launching with RCVR-1 selected. The XSDC receives too much noise when X-TWTA-2 is on, so the two can't operate together.

are identical to each other, and the two TMUs are nearly identical to each other.[11] The TMU and the RFS exciter are fully cross-strapped. Likewise, the CDU pair is cross-strapped with the RFS receiver pair and with the hardware command decoder of the CDS.

The TMU receives two serial data streams from the telemetry formatter of the CDS. The use of the uncoded 40-bps low-rate data has been reserved for when the spacecraft enters safing. The 10-bps to 134.4-kbps high-rate stream is convolutionally encoded[12] by the TMU. The TMU can modulate either the low-rate bit stream or the high-rate symbol stream on either a 22.5-kHz subcarrier or a 360-kHz subcarrier from an internal TMU oscillator. TMU-B can provide the symbol stream directly to the exciter (TDRSS mode).

The CDU receives a modulated 16-kHz command subcarrier from the RFS receiver. Depending on the ground station command mode, the subcarrier may be unmodulated, or modulated with a bit-synchronization (bit-sync) waveform equivalent to an all-zeroes command data stream, or with both bit-sync and command bits.

The CDU demodulates the command subcarrier. It provides three separate outputs to the CDS command decoder:

- A CDU in-lock or out-of-lock indicator
- The 32-bps command-bit timing (“clock”)
- The command bits.

2.4 S-/X-Band Antenna Subsystem

The SXA consists of an HGA[13] and two LGAs (LGA-1 and LGA-2). The two LGAs work at S-band only. The HGA was designed to work at S-band and X-band. Because the LGAs have no X-band capability, uplink or downlink at X-band requires the HGA. The spacecraft can be configured (via real time or sequenced commands) to receive and transmit S-band on the HGA, on LGA-1, or on LGA-2. The same antenna must be used for both reception and transmission of S-band at a given time. Galileo S-band antennas are right circularly polarized (RCP), simplifying the task of configuring the DSN. The X-band downlink polarization is RCP or left circularly polarized (LCP) depending which of the X-TWTAs is powered on.

The S-band antennas operate at a nominal uplink frequency of 2115 MHz and a nominal downlink frequency of 2295 MHz. The actual frequencies are DSN channel 18 for RFS receiver 1 (and for a two-way coherent downlink with that receiver) and channel 14 for RFS receiver 2 (and its coherent downlink) or a USO-generated downlink [2].

---

[11] The TMUs are almost identical. They differ as follows: TMU-A has an experimental “coder-2” that can produce a (15,1/4) convolutional code for 115.2 kbps and 134.4 kbps and modulate the coder-2 symbols on a 720 kbps subcarrier. TMU-B has a “TDRSS mode” wherein symbols from the (7,1/2) coder directly modulate the S-band carrier (no subcarrier). Adding the experimental coder less than 2 years before launch was a result of the delay in launch date from 1982 to 1989 and consequently the prime mission period to 1995-1997. The decrease in output from the already-fueled RTG power supply during the delay meant the TWTA would likely operate only in the low-power mode. Part of the communications shortfall was to be made up by using the more efficient (15,1/4) code; the remainder by planning an array of the DSN’s 70-m antenna with the Very Large Array (VLA) radio science antenna system for the critical encounter data[4]. See [11] for a description of the use of the VLA as an arrayed antenna resource during the Voyager mission.

[12] See Section 4, **S-band Mission**, for a description of the “concatenated coding” used since 1996.

[13] The Galileo HGA did not deploy fully and therefore has never been functional for use in the mission. The antenna description in Section 2.4 is of the system as built and *intended* for use. See Section 4, **Galileo S-band Mission**, for the workarounds developed during flight to enable a successful mission.

Because the most prominent part of the HGA is a main reflector 4.8 m in diameter, it looks like a single antenna. However, the HGA has two separate feed systems, one for S-band and the other for X-band. In its functions, the HGA can in many ways be considered as two distinct antennas (S-HGA and X-HGA). The X-band and S-band boresights (direction of maximum gain) are co-aligned in the direction of the LGA-1 boresight, which is the –z axis.

Though this was not the original plan, LGA-1 has been selected for most of the mission. LGA-2, with its boresight aligned in the opposite direction from the LGA-1 boresight, was only used at specific times when the trajectory geometry required: Venus flyby and Earth-1 flyby (see Operational Scenarios).

In addition to LGA-1, LGA-2, and HGA, the orbiter also has two other antennas that are not considered parts of the orbiter telecom system. These are the relay receiving antenna (RRA) for the Galileo probe-to-orbiter relay link and the plasma wave spectrometer (PWS) antenna, part of a science instrument.

2.5 X- to S-Band Downconverter

The Galileo project has always considered the orbiter's single XSDC as an experimental subsystem, meaning that use of an X-band uplink isn't essential for receiving commands or other critical mission functions. The XSDC parts are

- Downconverter
- S-band coupler
- X-band diplexer
- Low pass filter
- Voltage controlled oscillator (VCO) coupler.

The X-band diplexer allows simultaneous X-band reception (via the XSDC) and transmission (via the X-band TWTA) through the HGA. The S-band coupler connects the down-converted X-band modulated carrier to RFS S-RCVR-1. Working with the RFS receiver and transmitter, and depending on the controlled configuration, the XSDC provides the telecom system with non-coherent or two-way coherent carrier operating modes with an X-band uplink.

2.6 Telecom Hardware Performance During Flight

The orbiter was launched with the following elements active: S-RCVR-1, S-EXC-1, S-TWTA-1, CDU-A, and TMU-A. The USO was turned on a few weeks after launch. As of the posting of this article in 2002, the originally selected units are still selected and generally operating without a problem.

The telecom hardware problems that have occurred during flight are

- HGA failure to deploy (discussed separately in Sections 4 and 6)
- RFS receiver "wandering VCO anomaly"
- Unexpected CDU lock-count changes
- USO frequency drift rate changed by radiation.

2.6.1 "Wandering VCO" RFS Receiver Incident

Several days after Ganymede-2, the second of the 10 Jovian satellite encounters of the prime mission, the orbiter receiver failed to acquire a routine uplink from the Madrid tracking

station on September 11, 1996.[14] Spacecraft turns, 90 deg off Earth and back, occurring several hours before the incident, may or may not have been relevant. Examination of the VCO volts telemetry by telecom showed the measurement had deviated by as much as –8 kHz and +24 kHz from best lock prior to the acquisition attempt [6]. The station acquired the uplink using a resweep frequency range 2.5 times as wide as standard. Over the next several days, tracking stations had to use sweep frequency ranges as much as 7.5 times the standard.

The receiver returned to normal operation after an RFSTLC (radio frequency subsystem tracking-loop capacitor) test. RFSTLC tests, conducted periodically through the prime mission, required a station to sweep its transmitter in frequency to pull the VCO to either +65 kHz or –65 kHz from the best-lock frequency (BLF), then to turn the transmitter off. The VCO frequency then relaxed back to BLF; the time it took to do so provided a measure of the time constant of the resistor-capacitor network in the tracking loop. In the first RFSTLC test after the incident, the frequency-change-vs.-time signature and the loop time constant were not normal. However, the VCO wandering stopped, and subsequent RFSTLC tests were normal in all respects. This receiver operated normally through the remainder of the prime and GEM missions and so far in GMM, with no recurrence of the wandering signature.

Ground testing and analysis focused on the receiver tracking-loop integrator, an LM108 operational amplifier. A model [7] that involves ionic contamination by sodium ions (Na+) fits the inflight data well, including the evident self-healing (“annealing”). No further receiver problems have occurred to date.

2.6.2 Unexpected CDU Lock-Count Changes

As part of its normal operation, the CDU increments a software counter each time it changes to or from out-of-lock to subcarrier-lock or subcarrier-lock to bit-sync-lock. The spacecraft telemeters the count as engineering data periodically. The CDU passes command data to the command decoder in the CDS only when it is in bit-sync lock. The number of lock counts for each session of planned commanding is known. If the count exceeds the predicted number, this is defined as an “unexpected CDU/CDS lock-count change.” These unexpected lock counts have occurred on Voyager and other projects, and have never caused any problem with commanding. The several unexpected lock-change events per year on Galileo place no restrictions on commanding activities. With greatly reduced engineering telemetry sample rates and telecom staffing in GEM and GEM, unexpected lock-count events are no longer analyzed, though they presumably still occur. There is no evidence of any change in receiver or CDU command performance since launch.

On Galileo, prime-mission unexpected lock counts have occurred from a variety of station configuration and operational problems [7]. Also, one repeatable spacecraft cause is known, having been verified in ground tests of a Galileo receiver and CDU in the early 1990s. During the test, one pair of lock changes occurred as a result of the combination of (a) the uplink tuning rate at the initial uplink acquisition by the unmodulated carrier at the start of a pass, (b) the uplink signal level of the unmodulated carrier, and (c) the relative frequency rate between the sweep and the receiver VCO. The effective frequency rate in the test included the combined effect of Doppler frequency at the receiver and the “random walk” frequency of the VCO.

[14] A Galileo uplink acquisition requires the station to turn on its 100-kW S-band transmitter and perform a frequency sweep. A standard sweep varies the frequency at a specified rate over a range of ±12 kHz about a center frequency, returning to the center frequency for the rest of the pass. Even with Doppler over a pass, this center frequency reaches the spacecraft near enough to the “best lock frequency,” the frequency the receiver VCO oscillates at without an uplink.

The "U/L ACQ (uplink acquisition) sweep" mechanism results in a waveform momentarily at the RFS receiver output to the CDU, which the CDU in turn interprets (in error) as bit sync command modulation. This waveform occurs when the frequency difference is about 512 Hz, the same as the Galileo command subcarrier frequency. The CDU sends an "in-lock" signal to the CDS, which records it as a lock-count change. After a moment, the RFS receiver output waveform is different, the CDU no longer interprets it as a command signal, and it sends an "out-of-lock" to the CDS. The CDS makes another lock count, for a total of two.

2.6.3 USO Radiation-Induced Frequency Offset and Rate Change

The USO is of Voyager project inheritance. Though each S-EXC has an internal auxiliary oscillator (aux osc), the USO has been the predominant non-coherent downlink carrier frequency source since it was turned on December 5, 1989. The USO was turned off for a few tens of days in late 1991 and once again in early 1992 in support of the anomaly investigation of the HGA failure to deploy.

The frequency of the crystal oscillator in a USO changes with time (ages). The multi-mission navigation team accounts for the relative velocity between station and spacecraft in their orbit determination and predictions of one-way Doppler frequency. Frequency shifts not accounted for in the navigation orbit-determination process can be used to ascertain other effects, such as the crystal aging or the effects of radiation.

It was also known, from Voyager's one-way Doppler profiles before and after the Voyager spacecraft flybys of Jupiter in 1979, that the Galileo USO frequency rate would be affected by the radiation dose at each planetary encounter. For the prime mission, the effect was qualitatively expected to be greatest at JOI, because the largest radiation dose occurred there. However, the Voyager experience could not be confidently carried over to make a quantitative prediction of the radiation-induced USO frequency change for Galileo. Based on the Voyager experience, the project and the DSN coordinated, as part of the overall JOI telecom strategy, to search for and quickly find the one-way downlink.

The radiation-induced USO frequency changes have continued through the Jupiter encounters of the prime, GEM, and GMM missions. The offset changes are usually fairly small (less than 5 Hz at S-band over a couple of days) at each encounter.[15] The pre-encounter drift (aging) rate has been observed to resume as the orbiter returns to greater distances from Jupiter. To ensure rapid lockup by the ground receiver, the DSN sends out periodic USO frequency update messages (known as TFREQ updates) for use in tracking operations whenever the USO frequency (referenced to S-band) has changed by more than 0.5 Hz.[16]

---

[15] On November 5, 2002, the Galileo orbiter will fly past the satellite Amalthea at a distance of less than 1 R_J above Jupiter's cloud tops. The radiation level predicted for this flyby is significantly greater than that during JOI. The total dose is estimated to be 2.5 times that incurred during a typical Io flyby. The project is planning on how best to configure the orbiter's flight software (including fault protection algorithm updates) to survive this radiation.

[16] On December 11, 2001 and again on January 27, 2002, the received downlink frequency in the one-way mode exhibited rapid and unexpected variations of several tenths of a Hz. These fluctuations, thus far unexplained, occurred over more than one 70-m station. They each resulted in the loss of several frames of telemetry data when the station receiver carrier loop was unable to follow the rapid frequency changes. After a period of several hours, the downlink frequency became stable again, though at an offset of several tenths of a Hz from before each episode. Because the Sun-Earth-spacecraft angle was greater than 90 deg and the Sun was not unusually active, solar effects on the S-band downlink are ruled out. The episodes did not occur when the orbiter was in a high-radiation region. By elimination of other possible causes, the circumstances point to the USO or its control circuitry as a source of the frequency fluctuations, but not to a specific cause.

2.7 Orbiter Input Power and Mass Summary

When operating, each telecom system element has a single power input mode except for the TWTAs, which have both high-power and low-power modes. Table 2-2 summarizes the steady-state spacecraft input power and the RF output power for both high-power and low-power modes, as applicable. The table also summarizes the masses of components of the system.

Table 2-2. Galileo orbiter input power and mass summary.

	Number of Units	Input Power (W)[a,b]	Output Power (W)[c]	Mass (kg)[a,d]
RFS				53.5
Transponder	2			
Receiver		4.5		
S-band exciter		2.6		
X-band exciter		3.5		
ACIS[e]	1	0.7		
USO	1	2.7/4.5		
X-band TWTA	2	46.9/72.4	11.6/20.0	
S-band TWTA	2	34.9/87.1	4.9/14.8	
DOR		1	0.5	
XSDC	1	3.1		2.5
MDS				9.8
CDU	2	4.4		
TMU	2	5.5/5.8		
SXA				
Deployment motor		2	12.0	
Antenna[f]				8.1

[a] Mass is from [2], module GLL-3-230; input power is from [2], module GLL-3-250.

[b] For TWTAs, the smaller power value is for low-power mode, the larger for high-power. For USO and TMU, the lower value is near-Earth, and the larger is at Jupiter.

[c] RF power defined as design value at RFS/SXA interface (LGA-1 for S-TWTA and HGA for X-TWTA).

[d] The stated mass is the total for the subsystem (for example, 9.8 kg for the MDS includes 2 TMUs and 2 CDUs).

[e] Antenna control and interface system.

[f] Mass does not include antenna structural elements. The entire orbiter structure is 255.5 kg.

Section 3

Ground System

The DSN* is an international network of ground stations (antennas, transmitters, receivers, and associated systems) that operates intensively at S-band and X-band, and with a Ka-band capability being developed.[1] The DSN supports interplanetary spacecraft missions and radio and radar astronomy observations for the exploration of the solar system and beyond. The DSN consists of three deep-space communications complexes located approximately 120 deg from each other at Goldstone, in California's Mojave Desert, near Madrid, Spain and near Canberra, Australia. Each complex has one 70-m antenna, two or more 34-m antennas, and one 26-m antenna (not used for Galileo).

Specific DSN numerical parameters for Galileo are defined in DSN Operations Plan for the Galileo project [8]. During the prime orbital mission (December 7, 1995 through December 7, 1997) Galileo used the 70-m stations standalone, and in arrays with the 34-m stations in operation at the time. During the GEM and GMM, Galileo has returned to using the 70-m stations standalone. *The Deep Space Mission Systems (DSMS) Telecom Link Design Handbook* [9] includes functional capability descriptions of each antenna type for the purpose of modeling link capability between a spacecraft and station.[2, 3]

3.1 Uplink and Downlink Carrier Operation

Though the spacecraft was designed and built to use both S-band and X-band uplinks and downlinks, Galileo uses only the S-band links.

---

* Look up this and other abbreviations and acronyms in the list that begins on page 63.

[1] See http://deepspace.jpl.nasa.gov/dsn/brochure/index.html, an online "brochure" about the DSN, including its history, the three deep space communications complexes, and brief descriptions of the DSN's antennas, receivers, station arrays, and telemetry decoding.

[2] Reference [9] is http://eis.jpl.nasa.gov/deepspace/dsndocs/810-005/, document 810-005 (Rev. E), released January 2001. The Galileo spacecraft was originally designed to work with ground systems defined in the previous version of the Handbook [10], known as 810-5 (Rev. D). This description of 70-m station antenna and microwave systems, BVR, command processing, and telemetry processing, is consistent with 810-005, Rev. E.

[3] See http://www.jpl.nasa.gov/basics/bsf18-3.html for a general description of uplink and downlink data flow at a Deep Space Communications Complex.

Figure 3-1 shows the antenna and microwave sections of a 70-m station, and the following paragraphs describe Galileo-related functions of that type of station. Refer to [9] for corresponding figures and descriptions of the other types of DSN stations.

3.1.1 Uplink

The 400-kW high-power S-band transmitter at the 70-m site, operated at 100 kW, supports Galileo communications at Jupiter distance on the LGA. Galileo has not used the 20-kW low-power S-band transmitter since interplanetary cruise.

The uplink carrier, modulated with a command subcarrier when required, goes through an S-band diplexer, orthomode junction and polarizer to the S-band feed. From there, as Fig. 3-1 shows, the uplink path is via three smaller reflectors and the 70-m reflector before radiation to the spacecraft.

3.1.2 Downlink

From the 70-meter reflector, the S-band downlink is directed by the subreflector to the S/X dichroic reflector. A dichroic surface is reflective at one frequency band and transparent at another, thus allowing the S-band frequencies to be separated from X-band frequencies for individual processing. The dichroic reflects the S-band downlink to the path shown by the thick line in Fig. 3-1 to the S-band feed. Reversing the path taken by the uplink, the downlink is directed by the diplexer to an S-band maser preamplifier, and its frequency is down-converted for input to the block V receiver (BVR) and the Deep Space Communications Complex (DSCC) Galileo telemetry (DGT) system.

3.2 Command Processing

The JPL Galileo spacecraft mission controller, referred to as the ACE, operates the multi-mission command system from a workstation in the mission support area (MSA). The ACE transfers command files from the Galileo MSA to the DSCC minutes in advance of transmission in a store-and-forward process. At the DSCC, the command processor assembly (CPA) and the command modulator assembly (CMA) clock out the command bit stream, modulate the command subcarrier, and provide the subcarrier to the station’s exciter for modulation of the RF uplink carrier. The command bit rate is set by the ACE. The command subcarrier frequency and modulation index (suppression of the uplink carrier) are controlled through standards and limits tables at the DSCC.

Just prior to a command session, the ACE directs the station to turn command modulation on and selects the Galileo 32 bps command rate and a calibrated buffer in the station’s CMA. The CMA produces the command subcarrier, which produces a 512 Hz squarewave to match the subcarrier tracking loop best lock frequency in the Galileo CDU. As the ACE sends the spacecraft commands, the CMA modulates the command bit waveform onto the subcarrier. When finished, the ACE directs the station to turn command modulation off.

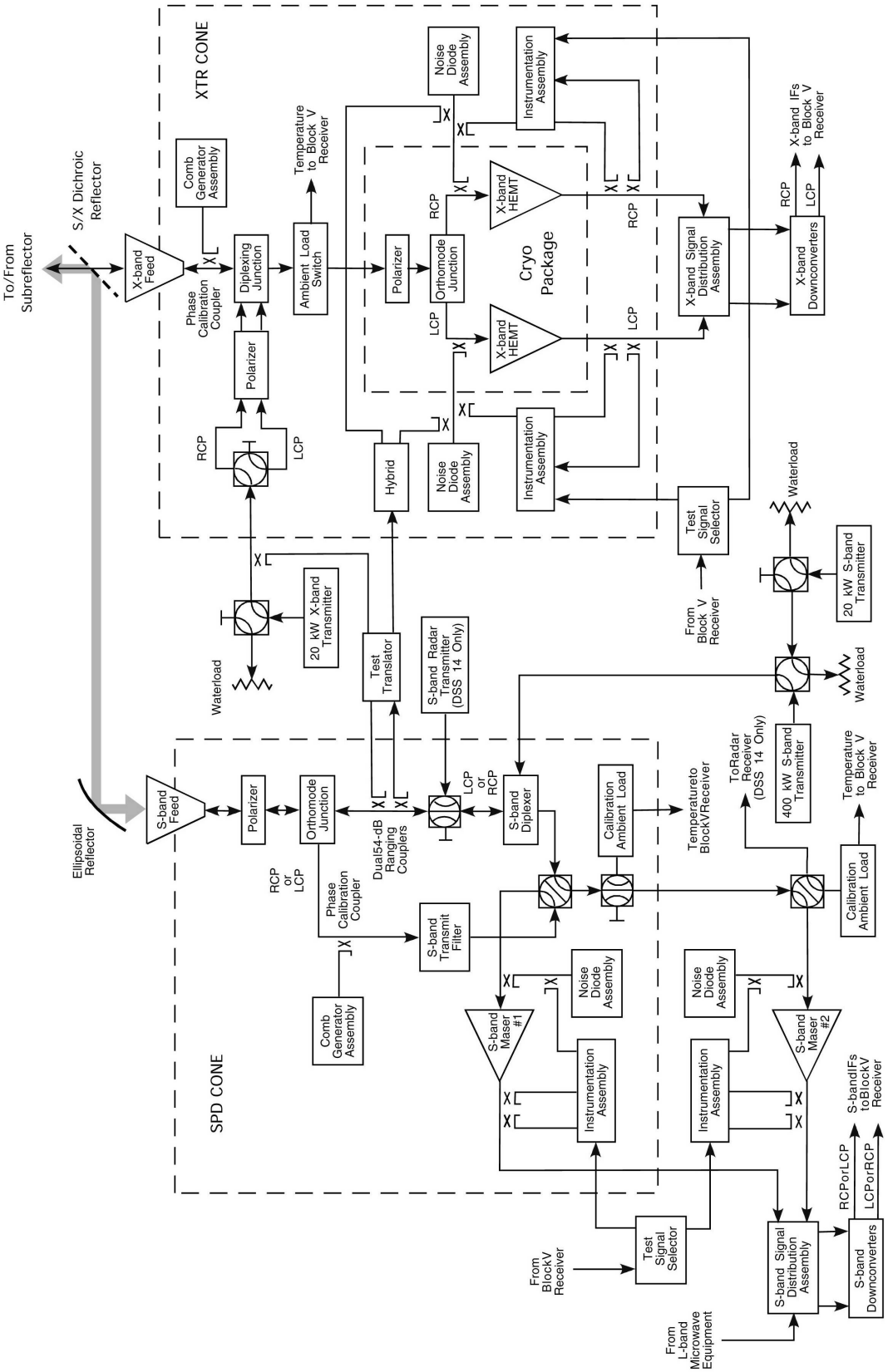

Fig. 3-1. DSS-14 and DSS-43 microwave and transmitter block diagram.

3.3 Telemetry Processing

During interplanetary cruise from 1989 to 1995, telemetry processing from the Galileo residual carrier downlink was conventional, the same as used for Voyager [11] and other deep space missions of the era. Bit rates as high as the maximum 134.4 kbps available from the spacecraft were supported via LGA-1 or LGA-2 during the Earth flybys when the spacecraft-station range was relatively small [12].

Section 4 describes the development, configuration, and operation of the telemetry system for the Galileo S-band mission; also known as the DGT (DSCC Galileo telemetry).

3.4 Radiometric Data

Throughout the mission the Galileo uplink and downlink carriers have provided a means of measuring the station-to-spacecraft velocity as a Doppler shift. In addition, during a portion of interplanetary cruise (before the S-band links through the LGA became too weak), ranging modulation applied to the uplink was turned around by the transponder to modulate the downlink to provide a means of measuring the station-to-spacecraft distance.

Figure 3-2 (from [10]) shows the metric-data assembly (MDA) for processing Doppler. The BVR provides downlink phase to the MDA, for Doppler measurement. When the spacecraft transponder is locked to an uplink carrier, the MDA compares the downlink phase to the uplink phase that was transmitted a round-trip light time (RTLT) earlier, for two-way Doppler. The Doppler measurements establish the spacecraft-station velocity as a function of time and can be compared with the expected or modeled velocity. The Doppler-sample rate for Galileo is normally 1 sample per 10 s but has been as high as 10 samples per s for encounters and radio science occultation experiments.

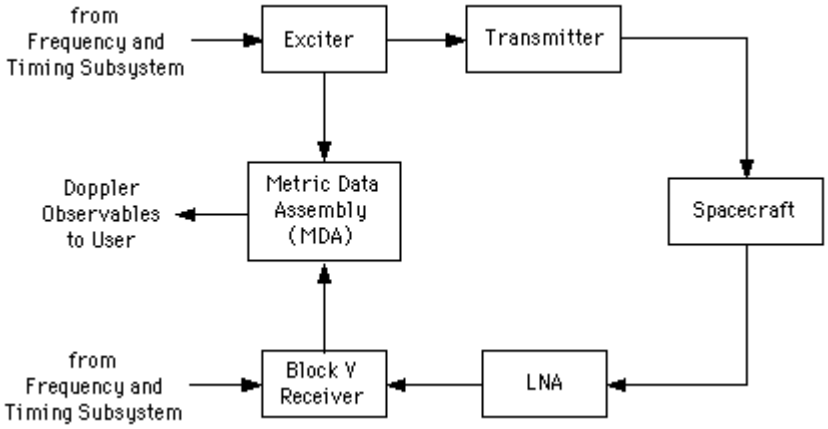

Fig. 3-2. DSN Doppler system for Galileo.

For the Galileo mission, the uplink-ranging data sent to the spacecraft and the ranging data demodulated from the downlink carrier were both processed in the sequential ranging assembly (SRA).

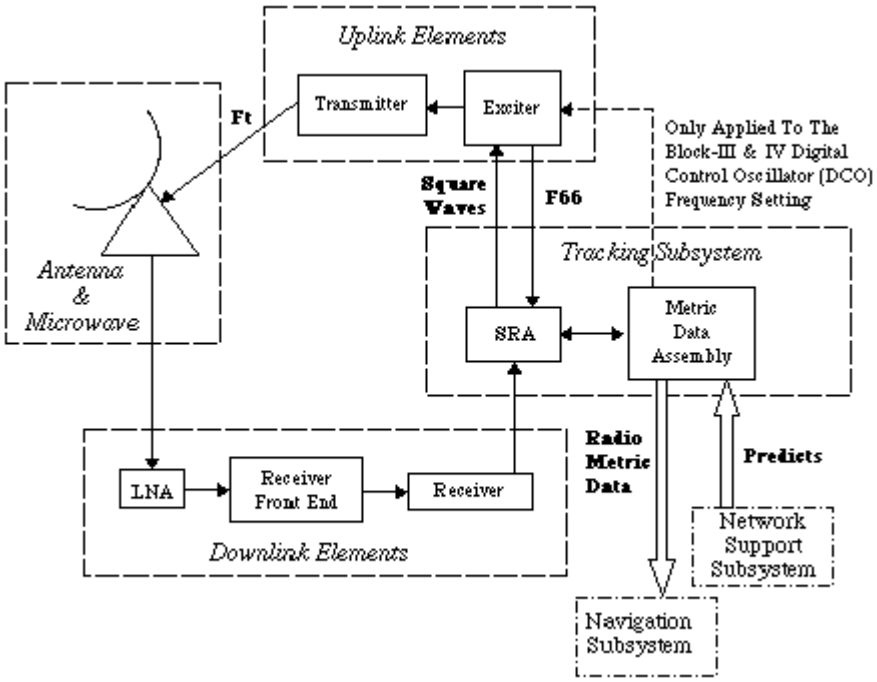

Fig. 3-3. DSN ranging system for Galileo.

The name refers to the sequence of square-wave frequencies sent to the spacecraft, with the highest frequency ("clock") providing fine resolution in range. Square-wave frequencies, at successive submultiples of the clock, resolve ambiguity.[4] To accommodate the decreasing link margins as Earth-orbiter range increased in the latter part of interplanetary cruise, Galileo used a 126-s integration time for the clock component and 14-s integration time for the lower-frequency components. Galileo ranging used components 4 through 9 for ambiguity resolution [8].

[4] The process of ranging involves correlation between the transmitted and received waveforms. The correlation results in an infinity of solutions, separated one wavelength apart, creating the ambiguity. The ranging system resolves (eliminates) the ambiguity by successively correlating a series of waveforms, each one having a wavelength twice as long as the previous, until the spacecraft's location is unambigous as determined by means other than the current range measurement.

Section 4

Galileo S-Band Mission

4.1 Overview

This section describes the extraordinary collaboration effort between a reconstituted Galileo project software development team, the Galileo flight team, and the DSN* technology development team that saved the Galileo Mission from the high-gain antenna failure and eventually led to the overall success of the Galileo mission. This effort was made the subject of a DSN Advanced Systems Program[1] case study [13].

During its early cruise phase, the Galileo orbiter communicated with Earth using the S-band signals from the LGA. As designed for thermal control, the HGA "umbrella" antenna with X-band capability was to remain furled until the Sun-spacecraft range became and remained greater than 0.9 AU before the second flyby of Earth. On April 10, 1991, about 1-1/2 years after launch and with the thermal constraint lifted, the orbiter was commanded to turn the HGA deploy motors on to unfurl its HGA. The antenna failed to fully deploy. Analysis of telemetry data and pre-launch design and test data pointed to a scenario that 3 of the 18 ribs of the umbrella antenna remained stuck to the antenna's central tower. Several unsuccessful attempts were made to free the stuck ribs. Because the reflector had not achieved a parabolic shape, the antenna was not functional. The only way to continue communicating was through the use of the Earth-facing LGA-1. And if the then-current configuration (ground and spacecraft) remained unchanged, the telemetry data rate would decrease to 10 bps by JOI. The originally planned X-band HGA downlink data rate was 134.4 kbps.

For over a year, much thought was expended in ground testing and analysis, leading to multiple efforts to free the stuck ribs. Most attempts involved turning the spacecraft toward and away from the Sun, in the hope that warming and cooling of the antenna assembly would free the ribs through thermal expansion and contraction. These attempts were unsuccessful. Other analysis suggested that turning the antenna deployment motors on and off repeatedly

* Look up this and other abbreviations and acronyms in the list that begins on page 63.

[1] The names of the program and the organization have changed since this work was done. The DSN is now part of the Interplanetary Network Directorate at JPL. See http://deepspace.jpl.nasa.gov/ for details.

("hammering") might deliver enough of a jolt to free the sticking and open the antenna. Unfortunately this effort failed also. Other approaches were tried, but none of these worked. For example, the X-band downlink and uplink were operated through the partly deployed HGA to compare end-to-end capability with the S-band LGA-1 capability.[2]

In parallel with the efforts to unstick the HGA, the JPL Flight Projects Office (Galileo Project), the JPL Telecommunication Division, and the JPL Tracking and Data Acquisition Office supported a study from December 1991 through March 1992 to evaluate various options for improving S-band telemetry capability through LGA-1.[3] The study assumed that image and instrument data, as well as spacecraft calibration and monitoring data, would have to be heavily edited and compressed using the Galileo's onboard processors, which had severe limited computation and memory resources. The study also presumed significant science and mission replanning and major ground system improvements would also be necessary.

The Galileo S-band mission was formally approved and funded in January 1993. The concept involved substantial changes to both the spacecraft and the DSN. Some key communications technologies used are

- Intra-site and inter-continental antenna arraying, to increase the effective aperture by combining signals from up to six antennas
- S-band "ultracone" feed and low-noise amplifier at the Canberra 70-m station, to provide a receive-only very low system temperature
- Suppressed carrier tracking with the BVR, to improve modulation efficiency
- Advanced channel coding, to reduce the operating signal-to-noise ratio (SNR) threshold
- Low-complexity lossless and lossy data compression and image editing schemes, to reduce the onboard data volume without compromising the science objectives.

The first four items together, it was estimated, would increase the supportable downlink data rate by one order-of-magnitude, from 10 to about 100 bps on average.[4] Including the fifth, data compression, would provide another order-of-magnitude increase in performance.[5]

These expectations were achieved. With the improved S-band downlink, the orbiter was able to complete 70% of the objectives of the original primary mission. With continued use of

---

[2] Use of the HGA was found not viable. The test showed the X-band downlink, near the HGA boresight, had about 2 dB improvement relative to LGA-1 S-band downlink. The pattern had numerous deep nulls, suggesting that keeping the antenna sufficiently pointed would be a major operational challenge. Further, it wasn't known if the nulls might change position with time due to temperature changes or mechanical movement.

[3] As early as October 1991, the TDA Office chartered a 1-month study to identify a set of options to improve the telemetry performance of the Galileo mission at Jupiter, using only the LGA. At the end of the study, the four options recommended for further evaluation (arraying of ground antennas, data compression, advanced coding, and suppressed carrier downlink) eventually were all put to use in the S-band mission [4]. Note: this organization, parent to the DSN, was called the TDA in 1991; it later became the TMOD, and is the IND in 2002.

[4] Arraying would improve the downlink by up to 4 dB depending on which antennas were used, the ultracone would improve it by another 1.7 dB, suppressed carrier modulation by 3.3 dB, and advanced coding by 1.7 dB. Together with the corresponding spacecraft modifications including data compression, the ground enhancements would meet the S-band mission Project objective to return one full tape recorder load of data after each satellite encounter, as well as satisfying the Project requirement to receive continuous engineering data and low-rate science [4].

[5] Data compression reduces the transmission and storage bandwidth required by removing intrinsic redundancy in the source data, but leaving the transmitted data more vulnerable to communication channel errors. Error correction coding introduces structured redundancy to the data to reduce the effects of channel errors, incidentally increasing channel bandwidth. Data compression and coding, used together as in the Galileo S-band mission, can produce a large improvement in the end-to-end system efficiency.

the improved S-band downlink (except for arraying) in GEM and GMM, the orbiter has returned significant amounts of science data.

4.2 Ground System Improvements for Galileo S-Band Mission

The DSN changes involved various enhancements to the three DSCCs that could provide a factor of 10 increase in data return from the Galileo spacecraft as compared with the data return that would result from use of the existing DSN configuration receiving S-band via the spacecraft LGA-1 only. The design is shown in conceptual form in Fig. 4-1. It included the addition of the DGT, a new telemetry subsystem to serve as a signal processor, specifically designed to handle the Galileo low-signal conditions.[6] The S-band mission packet-telemetry, suppressed-carrier DGT mode (known in Galileo spacecraft flight software as "Phase-2") began in May 1996.[7]

4.2.1 DSCC Galileo Telemetry

The DGT was installed in parallel with the existing BVR and telemetry channel assembly (TCA), which formed a part of the DSN telemetry subsystem. The BVR and TCA continued to provide for Doppler extraction and spacecraft emergency support.[8] In 1995 the BVR was a new digital receiver for multi-mission support that was used for Galileo at Jupiter encounter. The BVR was capable of acquiring and tracking the spacecraft carrier in a residual or suppressed-carrier mode and of demodulating carrier, subcarrier, and symbols. For the Galileo S-band mission (Phase-2), the BVR delivered symbols to either the DGT's feedback concatenated decoder (FCD) in the packet mode or to the TCA's maximum likelihood convolutional decoder (MCD) in the time-division multiplexing (TDM) mode. Figure 4-1 shows the BVR interface to the FCD as developed for non-arrayed operation.

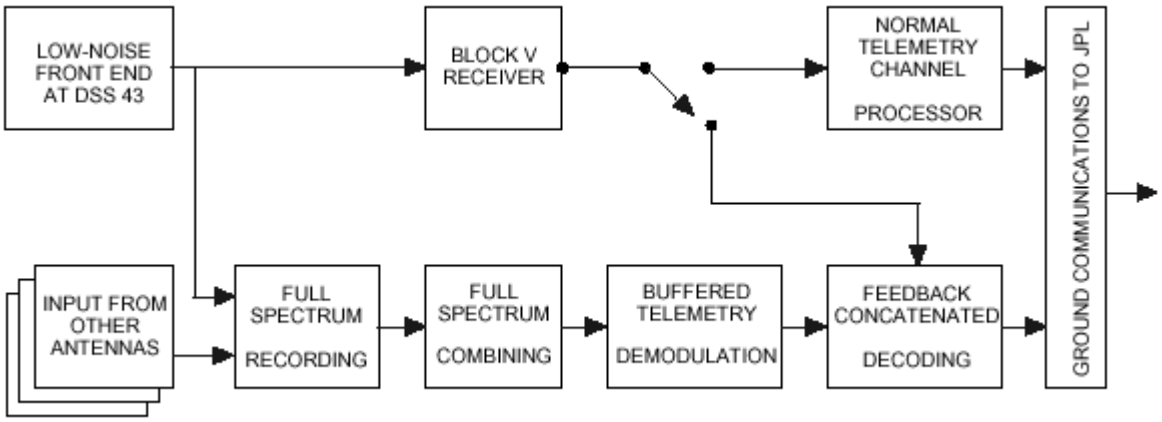

Fig. 4-1. Conceptual form of the DGT for Galileo.

---

[6] Material in this paragraph comes largely from [6]. The DGT includes a full-spectrum recorder (FSR), a full-spectrum combiner (FSC), the buffered telemetry demodulator (BTD, a receiver with phase-locked loops for carrier, subcarrier, and symbols), and a feedback concatenated decoder (FCD).

[7] To reduce the risk to the Galileo one-chance-only events from schedule slips in the new ground system development, Galileo planned the critical December 1995 Probe data return and JOI activities to operate using the existing spacecraft Phase-1 software and the existing telemetry system only. Section 6.6 describes Phase-1 and Phase-2.

[8] Through GEM and GMM, the S-band mission safemode continues to produce a residual carrier downlink, modulated by 40 bps "high-rate" TDM data with (7,1/2) convolutional encoding.

4.2.2 Ultracone at Canberra 70-m Station

In addition to the DGT, an ultra-low-noise receive-only feed system was added to the Canberra 70-m antenna to reduce the S-band system noise temperature to 12.5 K, excluding atmospheric effects. Prior to installation of this so-called "ultracone," Galileo operations had been conducted with an S-band polarization diversity (SPD) feed cone having system noise temperatures at zenith of 19.9 K in the diplexed transmit/receive mode and 15.6 K in the receive-only mode, both excluding the effects of the atmosphere. The ultracone met its system noise temperature (SNT) design objective. It continues to be used in the GMM, with a total system noise temperature (including atmospheric effects) of about 15 K at high elevation angles in good weather.

4.2.3 Arraying Ground Antennas

Further enhancement of the Galileo downlink signal was obtained through the following antenna-arraying techniques at the Canberra CDSCC:

- Intercontinental arraying of the 70-m antenna at the Goldstone, California, with the 70-m antenna near Canberra, Australia, during mutual view periods
- Addition of two of the three 34-m antennas at Canberra into the array with the 70-m antennas at Canberra and Goldstone
- Addition of the Australian 64-m radio telescope at Parkes into the array. Parkes, called Deep Space Station 49 (DSS 49), for DSN identification, supported the Galileo mission as an additional element of the Canberra array.

The timeline for arraying was generally: (a) begin the array, as Canberra "rises", by adding the Canberra 70-m and two 34-m antennas to the Goldstone 70-m antenna already tracking, (b) add Parkes about 2 hours later,[9] (c) then delete the Goldstone 70-m antenna as it sets, and (d) finally, delete Parkes as it sets about 2 hours before the Canberra array sets.

NASA provided several enhancements to the Parkes radio telescope to increase its contributions to the array.

The overall network configuration used to support this phase of the Galileo mission is shown in Fig. 4-2. At each antenna, the S-band signal from the spacecraft was converted to a 300-MHz intermediate frequency (IF) by an open-loop downconverter. The IF outputs went simultaneously to the BVR channel and the DGT's FSR channels.

[9] The Parkes antenna, with a minimum operating elevation angle of 30 deg, has a later rise time and an earlier set time than the Canberra antennas, with their minimum elevation angles of 6–8 deg.

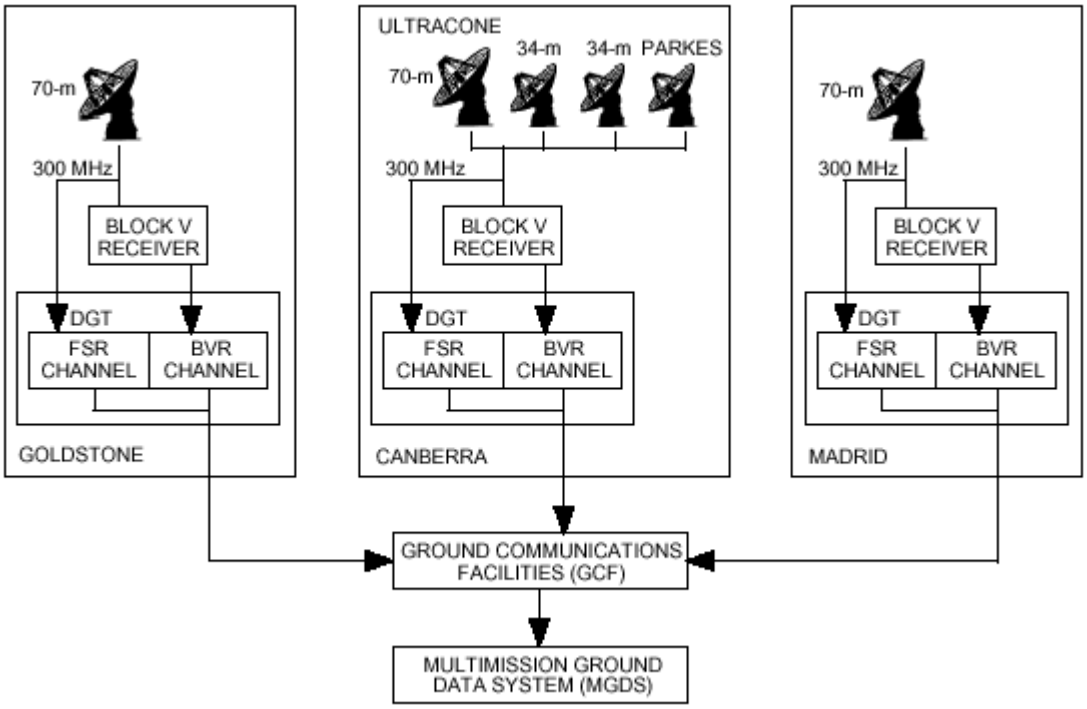

Fig. 4-2. DSN configuration for Jupiter orbital operations.

4.3 Data Compression

The objective of data editing and compression for both imaging and non-imaging data is the same: to reduce the number of information bits that need to be stored on the Galileo tape recorder and transmitted to the DSN.[10] One uncompressed Galileo image consists of 800 lines of 800 picture elements (pixels), with each 8-bit pixel defining one of 64 grey-scale levels.

The development of data compression for the S-band mission included several steps:

- Selection of a compression scheme
- Evaluation of acceptability of scheme by the scientists
- Development of compression ratio estimates for mission planning
- Post-processing techniques to remove artifacts without compromising accuracy.

Because the bulk of Galileo's data volume is imaging data, this article's description of data compression will use imaging data as an example.

4.3.1 Compression Scheme

The candidate scheme chosen for detailed evaluation and eventual implementation is the integer cosine transform (ICT) scheme for lossy image compression. ICT can be viewed as an integer approximation of the discrete cosine transform (DCT) scheme, regarded as one of the best transform techniques in image coding. Its independence from the source data and the availability of fast transform algorithms make the DCT an attractive candidate for this and other practical image-processing applications.

[10] The material in this section is largely from [14].

Data compression was to be accomplished in Galileo's onboard processors prior to the compressed data being recorded on the tape recorder. The processors are severely limited in computation and memory resources. The specific Galileo scheme uses an 8 × 8 ICT. The integer property reduces the computational complexity by eliminating real multiplication and real addition. The relationship between the ICT and DCT allows the use of efficient (fast) techniques that had been previously developed for DCT. Simulation of the Galileo ICT produced similar rate distortion results as a standard DCT scheme.[11]

4.3.2 Scientist Evaluation

Because the prime mission images and other Galileo data were expected to be of much higher resolution than data from the Voyager flybys of Jupiter, it was essential for the lossy data compression to preserve the scientific accuracy (validity) of the data. Two methods were used to achieve and maintain the required accuracy. First, the Galileo principal investigators (PIs) and other planetary scientists evaluated the effects of compression on the best previously available images. Second, small portions of images (named "truth windows") were to be stored and transmitted without lossy compression. The scientist-evaluation process, named "PI-in-the-loop visual evaluation," was done in collaboration with the Remote Payload Systems Research group and the Vision group at the NASA Ames center. The experiment, using sets of monochromatic astronomical images, converged rapidly on an acceptable set of customized quantization tables and verified the existence of compression/distortion trade offs acceptable for scientific evaluation [14].

4.3.3 Truth Windows

To ensure adequate accuracy, the concept of an addressable truth window (TW) was built into the image data compression. The TW is a fixed 96 × 96 pixel region that can be located anywhere in the 800 × 800 pixel image. To conserve onboard memory, the TW is losslessly compressed using the Huffman encoding module of the ICT compression algorithm, thus not requiring any additional onboard software. The PI can use the TW both to preserve important details and as a statistical reference to the rest of the image following application of image restoration techniques.

4.3.4 Compression Ratio Prediction Techniques

These techniques facilitate science and mission planning. For the Galileo fixed-to-variable compression scheme, an algorithm was given to the scientists. The algorithm predicts the compression ratio from a lookup table, based on the known statistics of the camera, the type of image expected, and its estimated entropy. The entropy, in terms of adjacent pixel differences, was modeled with a generalized Gaussian function with parameters based on previously available planetary images.

4.3.5 Post-Processing

Image restoration techniques had previously been used in other applications to remove the undesirable blockiness and checkerboard effects inherent in the output decompressed images produced by block-based transform compression schemes. However, the Galileo scientists' concern was that, while these techniques may make the image "look better," this is at the

[11] Rate distortion theory is used to compute the minimum bit rate required to transmit a given image, for a specified amount of distortion. The results can be obtained without consideration of a specific coding scheme. A summary of rate distortion theory is available in http://www.stanford.edu/class/ee392c/lectures/03._Rate_Distortion_Theory.pdf

expense of introducing distortions that reduce detail and thus compromise scientific accuracy. With this in mind, the Galileo post-decompression restoration techniques work first in the frequency domain, then in the spatial domain. Frequency coefficients are adjusted within the range of possible original values. Linear filtering is then performed with the constraint that frequency coefficients stay within their range of possible original values, creating a restored image that could be acceptably close to the original image.

4.4 Galileo Encoding and Feedback Concatenated Decoding

4.4.1 Overview

The Galileo S-band mission is supported by a coding system that uses an inner convolutional code concatenated with outer Reed-Solomon (RS) codes having four different redundancies.[12] To reduce the effects of error bursts, the interleaving depth is 8. Contrast this signal design with the original Galileo signal design for the HGA mission as defined in [2]. In that original design, the solid state imaging (SSI) imaging data was coded by a (255,241) RS code, with interleaving depth of 2, and the output of that code was convolutionally coded by the TMU.[13]

For the S-band mission, the staggered RS redundancy profile was designed to facilitate the novel feedback concatenated decoding strategy. Figure 4-3 is a block diagram of the Galileo FCD. The decoding process proceeds in four distinct stages of Viterbi decoding, each followed by Reed-Solomon decoding. The RS decoders use a time-domain Euclid algorithm to correct errors and declare erasures.[14] In each successive stage, the Reed-Solomon decoder tries to decode the highest redundancy codewords not yet decoded in previous stages, and the Viterbi decoder redecodes its data utilizing the known symbols from all previously decoded Reed-Solomon codewords.

The (14,1/4) convolutional code used for the Galileo mission is the concatenation of a software (11,1/2) code and the existing (7,1/2) code in the TMU hardware. The choice of this convolutional code was constrained to use the existing (7,1/2) code and by the processing speed of the ground decoder.

The Viterbi decoder portion of the FCD is implemented in software in a multiprocessor workstation with shared memory architecture. The use of a software decoder is possible due to the low downlink rate from the Galileo orbiter. The advantages of a software-based decoder are that its development cost is relatively low, and it provides the flexibility necessary for feedback concatenated decoding. To exploit parallel processing in multiple processors, the Viterbi algorithm uses “round-robin” frame decoding. In effect, this consists of running several complete, independent decoders for several frames in parallel. Compared with other approaches

---

[12] The material in this section is largely from [14] and [15]. The Galileo S-band mission error-correction coding scheme uses a (14,1/4) convolutional code as the inner code and a (255,*k*) variable redundancy RS code as the outer code. The RS codewords are interleaved to depth 8 in a frame. The redundancy profile of the RS codes is (94, 10, 30, 10, 60, 10, 30, 10). The generator polynomial, in octal, of the (14,1/4) code is (26042, 36575, 25715, 16723).

[13] From [2], module 3-300, *Telecommunications*, the orbiter was launched with two kinds of convolutional encoders. Besides the standard (7,1/2) encoder in each TMU, TMU-A also has an experimental (15,1/4) encoder. This coder could not be used for the LGA S-band mission because it was designed to operate only at 115.2 kbps or 134.4 kbps.

[14] The definition of an RS(*n*,*k*) code is one that accepts as input *k* data bytes and produces as a code word *n* bytes, where $n > k$. An RS(*n*,*k*) code can correct *t* errors and *s* erasures if $2t + s \leq n–k$. The Galileo codes are referred to as RS(255,161), RS(255,195), RS(255,225), RS(255,245).

considered, the round-robin requires minimum synchronization and communication because each processor is an entity independent of the others.

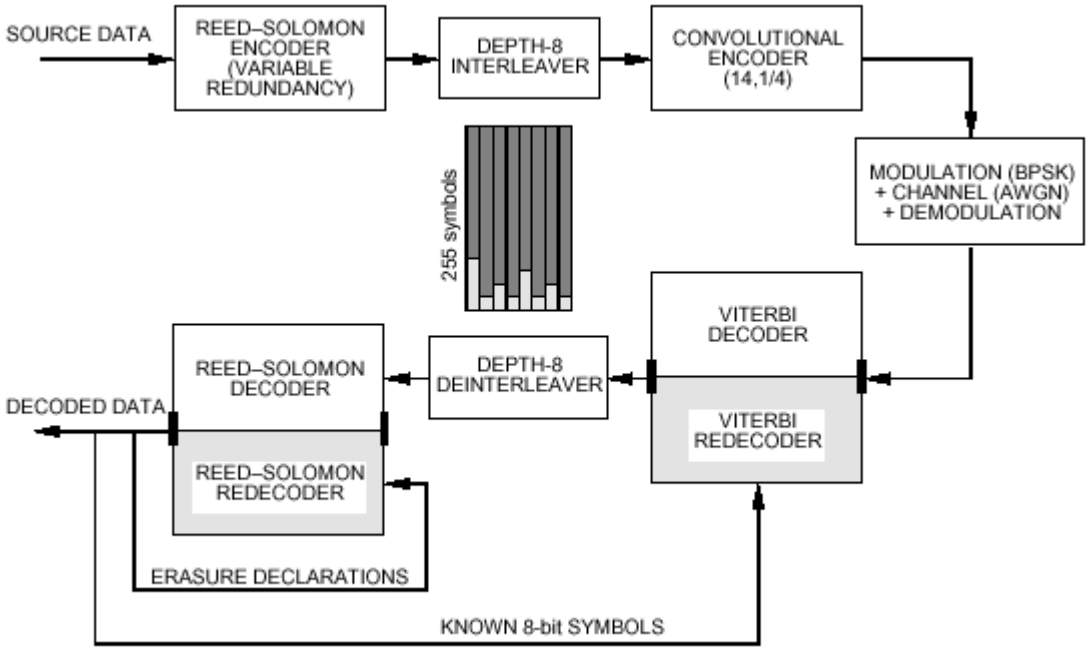

Fig. 4-3. Galileo encoding and feedback concatenated decoder.

4.4.2 Orbiter Coding and Modulation

An RS-encoded data block is interleaved to depth 8 and then encoded by the (14,1/4) convolutional encoder. The RS codewords can have four different levels of redundancies, as depicted by the lightly shaded areas at the bottom of the code block in Fig. 4-3. In the spacecraft, the encoded symbols are modulated on a subcarrier that modulates the downlink carrier. The deep space communications channel is characterized as additive white Gaussian noise (AWGN).

4.4.3 Ground Decoding and Redecoding

At the station (Fig. 4-2), the downlink carrier and subcarrier are demodulated by either a BVR or the DGT's own receiver, the buffered telemetry demodulator (BTD). Then, as shown in Fig. 4-3, the channel symbols from the receiver first go to a Viterbi decoder. After deinterleaving, the codeword or set of codewords with the highest redundancy is decoded by the RS decoder. If decoding of the first codeword is successful, the results (the "known 8-bit symbols" in Fig. 4-3) are fed back for Viterbi redecoding.

Redecoding facilitates Viterbi decoding. A correctly decoded RS bit forces the add-compare-select operation at each state to select the path that corresponds to the correct bit. The Viterbi decoder is thus constrained to follow only paths consistent with known symbols from previously decodable RS codewords. The Viterbi decoder is much less likely to choose a long erroneous path because any path under consideration is pinned to coincide with the correct path at the locations of the known symbols.

The RS-Viterbi decoding-redecoding process repeats for up to four times if necessary. In the first pass, only the first (strongest) code word RS(255,161) is decoded.[15] The symbols in the codewords decoded by the RS decoder are fed back to assist the Viterbi decoder to redecode the symbols in weaker codewords. At this and each successive stage, the output of the Viterbi redecoder is deinterleaved. In the second pass, the fifth codeword RS(255,195), which has the second highest redundancy, is decoded. The newly decoded symbols are fed back to further assist the Viterbi redecoder. The process is repeated twice more. In the third pass, the third and seventh codewords RS(255,225) are decoded, and finally in the fourth pass, the second, fourth, sixth, and eighth (weakest) code words RS(255,245) are decoded.

Figure 4-3 also shows a shorter feedback loop entirely within the RS decoder using erasure declarations.[16] If an RS byte error is detected but the byte can't be decoded, it can still be declared an erasure for future RS redecoding attempts. RS redecoding using erasure declarations based on error forecasting is worth about 0.19 dB when used in conjunction with one-stage decoding of the Galileo LGA convolutional code, shrinking to 0.02 dB with two-stage Viterbi decoding and almost nil with four-stage decoding [15].

Occasionally decoding remains unsuccessful even after four stages with two parallel FCDs, and the affected telemetry frame is declared lost.[17]

4.4.4 Control of Interaction Between Data Compression and Decoding Performance

By definition, data compression reduces the inherent redundancy in the source data. Loss of any packets of the compressed data from failure to decode causes a phenomenon called error propagation. How the error propagates depends on the compression schemes being used. The compressed Galileo data must be safeguarded against catastrophic error propagation.

The ICT scheme for Galileo imaging data includes a simple but effective error containment strategy. The basic idea is to insert sync markers and counters at regular intervals in the onboard data to delimit uncompressed data into independent blocks.[18] In case of ground packet loss or other anomalies, the decompressor can search for the sync marker and continue to decompress the rest of the data. For an 800-line × 800-pixel image before compression, the interval is eight lines. This error-containment strategy guarantees that error propagation will not go beyond 1% of the lines in an image.

---

[15] RS codewords are made up groups of eight bits, each called a "byte" or a RS symbol. RS symbols are not the same as the soft quantized communication channel symbols that are input to the FCD from the BTD or the BVR.

[16] This loop was implemented in the FCD but was not used operationally for Galileo.

[17] The open-loop downlink data (prior to BTD demodulation) is recorded to tape by the FSR. If high-value telemetry frames cannot be decoded in real time, the FSR tapes can be returned to JPL for labor-intensive non real time processing. Sometimes these frames can be successfully decoded after repeated attempts with different BTD or FCD parameter settings.

[18] The Galileo image error containment scheme works as follow. Every eight-line block of camera output is compressed into a variable-length compressed data block. The DC (steady-state bias) value is reset to zero at the start of every eight lines, thus making every eight lines independent. A 25-bit sync marker and a seven-bit modulo counter are inserted at the beginning of every eight lines. The chosen sync marker minimizes the probability of false acquisition to 10^{-8} in a bursty channel environment. In the ground decompressor, the error detection/sync software checks the prefix condition of the Huffman codes to detect any anomaly. When an anomaly is detected, decompression resumes from the next sync marker, and the reconstructed blocks are realigned using the modulo counter. The undecodable portion of the data is flagged and reported.

4.4.5 Concatenated Coding/Decoding Performance

Verification of the actual performance of the concatenated codes and interleaving that had been chosen by analysis required building the DGT. Because the orbiter packet-mode flight software was still in development, the DGT was tested with ground-generated signals during the year before deployment.[19] That testing verified an expected bit-energy-to-noise spectral density ratio (E_b/N_0) threshold of +0.6 dB (Viterbi decoder output), equivalent to a symbol-energy-to-noise spectral density ratio (E_s/N_0) threshold of –5.4 dB (BTD symbol output).

Downlink performance analysis in the GMM continues to show that the DGT decodes successfully at these levels. Empirically, the station monitor data shows that telemetry frames are lost (not decoded successfully in four passes through the decoder) rarely if the E_s/N_0 averages –6 dB or greater. Data rate planning for the S-band mission is now based on making data rate changes when the equivalent of the mean value of E_s/N_0 is at a level of –5.4 dB.[20]

[19] Data available at the time of the S-band mission studies in1991–1992 included [16] published in 1988. That paper referenced the effects of interleaving depth on concatenated system performance, including some test data for the (7,1/2) code. There was no in-depth analysis from which to extrapolate to the case of the (15,1/4) code. Simulation of concatenated system performance with the (15,1/4) code had not been feasible because of the amount of data needed to verify bit-error rates (BERs) even in the 10^{-5} to 10^{-6} range. One (15,1/4) simulation would have taken 30 hours of Sun-3/260 CPU time per 100,000 decoded bits.

[20] Section 5 describes the Galileo telecom link performance prediction process and provides signal level plots.

Section 5

Telecom Link Performance

This section describes the uplink and downlink predicted performance for the orbiter from December 1997 through August 2002. Communication link margins are computed using the link budget techniques and statistical criteria defined in *Deep Space Telecommunications Systems Engineering* [17]. Link performance is book kept using a design control table (DCT)*, an orderly listing of parameters from transmitter to decoder. The Galileo DCT includes favorable and adverse tolerances for each parameter that are used to determine a mean value and statistical variance for that parameter. As required by JPL link design policy[1] [18], overall performance is established in terms of the mean and the standard deviation (sigma).

Five link functions have been used during the mission: carrier tracking (Doppler), command, telemetry, turnaround ranging, and DOR. The functions still being used in the GMM are Doppler, command and telemetry.

The performance of each function is expressed as an SNR as shown in Table 5-1. The "noise" part of the SNR is expressed in terms of N_0, which is noise spectral density. The "signal" part of the SNR is P_c (carrier power), E_b (energy per command bit), E_s (energy per telemetry symbol), P_r (downlink ranging power), or P_{tone} (power in DOR tone). Each function has a minimum SNR, the threshold, at which the quality of the link meets the bit-error rate (BER) or other criteria defined by the project. The predicted SNR at all times must exceed the threshold SNR by a designated multiple of the standard deviation (sigma).

* Look up this and other abbreviations and acronyms in the list that begins on page 63.

[1] The link policy itself is posted at http://descanso.jpl.nasa.gov/index_ext.html

Table 5-1. Galileo orbiter telecom link functions and SNR criteria.

Function	SNR Definition	Galileo Criterion (designated multiple of sigma)
Carrier	P_c/N_0	Mean minus 3-sigma (UL), minus 2-sigma (DL)
Command	E_b/N_0	Mean minus 3-sigma
Telemetry	E_s/N_0	Mean minus 2-sigma
Ranging	P_r/N_0	Mean minus 2-sigma
DOR	P_{tone}/N_0	Mean minus 2-sigma

5.1 Design Control Tables

Predicted telecom performance for a typical configuration on March 19, 2002 is defined in Table 5-2 for uplink and Table 5-3 for downlink. These are DCTs produced by the telecom forecaster predictor (TFP) [19, 20]. TFP is a multi-mission tool for link performance prediction built upon Matlab. The Galileo TFP adaptation uses standard "common models" for station parameters, and Galileo spacecraft models.

The two DCTs show performance for a specific arbitrary instant in time, 2002-078/0:00 UTC, where 2002-078 is the day of year (DOY) corresponding to March 19, 2002. At that time, the Galileo spacecraft was being tracked with the 70-m station at Goldstone, DSS-14. The spacecraft was configured for S-band uplink and downlink on the LGA-1. The command rate was 32 bps, at an uplink modulation index of 0.571 radians. The downlink rate was 60 bps, at a modulation index of 90 deg.

5.1.1 Uplink Performance

Line 32 of Table 5-2, the mean command E_b/N_0, was 14.7 dB as compared with a threshold of 9.6 dB (line 33). Accounting for a 3-sigma variation of 3×0.74 (line 35), the command link had a margin of 2.89 dB (line 36).

5.1.2 Downlink Performance

Similarly, Table 5-3 shows the mean telemetry E_b/N_0 was 3.4 dB (line 42), the threshold is 0.6 dB (line 43), and the margin was 1.7 dB (line 46). This shows the link at 00:00 would support 40 bps telemetry at a criterion of mean minus 2-sigma.

5.2 Long-Term Planning Predicts

For planning spacecraft data-rate sequencing, TFP can produce tabulations or plots. While a DCT is a snapshot of many link parameters at one point in time, the tabulation (when read into a spreadsheet) can represent a whole series of snapshots. The rows represent successive points in time, and the columns represent values of individual parameters. Parameters can also be displayed as plots over a period of time.

For detailed data-rate planning, tabulations or plots can cover one station pass (8 to 12 hours) with points every 10 to 20 minutes. Figures 5-1 through 5-3 are plots of quantities during the DOY 2002-078 (March 19, 2002) DSS-14 pass just discussed. At another extreme, reasonably sized tabulations or plots can reach over spans of years with data spacing every 10 to 20 days. Figures 5-4 through 5-7 begin at the start of the GEM and continue through April 2002.

The plots appear on the seven pages following the DCTs, with brief interpretations beneath each plot.

Table 5-2. Galileo uplink DCT (DSS-14, 32 bps command) produced by GLL V1.1 10/04/1999.

Predict	2002-078T00:00:00.000 UTC
Up-/Downlink	Two-Way
RF Band	S:S
Telecom Link	DSS 14-Low Gain1-DSS 14
Command Uplink Parameter Inputs	
Command Data Rate, bps	32.0000
Command Modulation Index, rad	0.5710
Command Ranging Modulation Index, deg	0.0000
Mission Phase	Cruise
DSN Site	Gold-Gold
DSN Elevation	In View
Weather/CD	25
Attitude Pointing	MZ Pointed
External Data	
Earth-Craft Range, km	7.3012×10^{8}
Earth-Craft Range, AU	4.8806
Jupiter-Craft Range, km	1.9062×10^{7}
Jupiter-Craft Range, AU	1.2742×10^{-1}
Sun-Earth-Craft Angle, deg	96.82
Sun-Craft-Earth Angle, deg	11.19
Jupiter-Earth-Craft Angle, deg	1.08
One-Way Light Time, hh:mm:ss	00:40:35
Station Elevation, deg	56.67
Degrees-off-Boresight: LGA1, deg	0.81
Clock: LGA1, deg	0.00
Added S/C[a] Antenna Pointing Offset, deg	0.00
DSN Site Considered:	DSS-14/DSS-14
At Time:	0.00 hours after the start time

[a] Spacecraft.

Table 5-2. Galileo uplink DCT (DSS-14, 32 bps command) (cont'd).

Link Parameter	Design Value	Fav Tol[a]	Adv Tol[b]	Mean Value	Var[c]
Transmitter Parameters					
1.Total Transmitter Power, dBm	80.00	–0.50	0.50	80.00	0.0417
2. Transmitter Waveguide Loss, dB	–0.30	0.02	–0.02	–0.30	0.0001
3. DSN Antenna Gain, dBi	62.70	0.20	–0.20	62.70	0.0067
4. Antenna Pointing Loss, dB	–0.10	0.10	–0.10	–0.10	0.0017
5. EIRP[d] (1+2+3+4), dBm	142.30	0.67	–0.67	142.30	0.0501
Path Parameters					
6. Space Loss, dB	–276.22	0.00	0.00	–276.22	0.0000
7. Atmospheric Attenuation, dB	–0.04	0.00	0.00	–0.04	0.0000
Receiver Parameters					
8. Polarization Loss, dB	–0.16	0.10	–0.10	–0.16	0.0033
9. S/C Antenna Pointing Control Loss, dB	0.00	0.00	0.00	0.00	0.0000
10. Degrees-off-boresight Loss, dB	–0.03	0.51	–0.53	–0.04	0.0915
11. S/C Antenna Gain (at boresight), dBi	6.92	0.51	–0.53	6.91	0.0451
12. Lumped Circuit Loss, dB	–3.64	0.73	–0.82	–3.69	0.2002
Total Power Summary					
13. Total Received Power (5+6+7+8+9+10+11+12), dBm	–130.94	–1.87	1.87	–130.94	0.3902
14. Noise Spectral Density, dBm/Hz	–168.42	–0.73	0.65	–168.44	0.0792
15. SNT, K	1042.78	–160.84	168.42	1045.31	4518.08
16. Received P_t/N_0 (13–14), dB-Hz	37.51	2.06	–2.06	37.51	0.4694
Carrier Performance					
17. Command Carrier Suppression, dB	–1.50	0.10	–0.10	–1.50	0.0017
18. Ranging Carrier Suppression, dB	0.00	0.00	0.00	0.00	0.0000
19. Carrier Power (AGC[e]), dBm	–132.44	–1.88	1.88	–132.44	0.3919
20. Carrier Power Threshold, dB	–149.00	0.00	0.00	–149.00	0.0000
21. Carrier Power Margin (19–20), dB	16.56	1.88	–1.88	16.56	0.3919
22. Received P_c/N_0 (16+17+18), dB-Hz	36.01	2.06	–2.06	36.01	0.4711
23. Carrier Loop Noise Bandwidth, dB-Hz	10.86	–0.26	0.21	10.84	0.0180
24. Carrier Loop SNR (CNR[f]) (22–23), dB	25.17	2.10	–2.10	25.17	0.4891
Command Performance					
25. Command Data Suppression, dB	–5.34	0.00	0.00	–5.34	0.0000
26. Ranging Data Suppression, dB	0.00	0.00	0.00	0.00	0.0000
27. Received P_d/N_0 (0+25+26), dB-Hz	32.16	2.06	–2.06	32.16	0.4694
28. 3-Sigma P_d/N_0 (27–3×sqrt(27var)), dB-Hz	30.11	0.00	0.00	30.11	0.0000
29. Data Rate, dB-Hz	15.05	0.00	0.00	15.05	0.0000
30. Available E_b/N_0 (27–29),dB	17.11	2.06	–2.06	17.11	0.4694
31. Implementation Loss, dB	–2.40	0.50	–0.50	–2.40	0.0833
32. Output E_b/N_0 (30+31), dB	14.71	2.23	–2.23	14.71	0.5527
33. Required E_b/N_0, dB	9.59	0.00	0.00	9.59	0.0000
34. E_b/N_0 Margin (32–33), dB	5.12	2.23	–2.23	5.12	0.5527
35. E_b/N_0 Margin Sigma, dB	0.00	0.00	0.00	0.74	0.0000
36. E_b/N_0 Margin–3-Sigma (34–3×35), dB	0.00	0.00	0.00	2.89	0.0000
37. No Uplink BER model for GLL	NaN				

[a] Favorable tolerance.
[b] Adverse tolerance.
[c] Variance.
[d] Effective isotropically radiated power.
[e] Automatic gain control.
[f] Carrier-to-noise ratio.

Table 5-3. Galileo downlink DCT (DSS-14, 60 bps telemetry) produced by GLL V1.1 10/04/1999.

Predict	2002-078T00:00:00000 UTC
Up-/Downlink	Two-Way
RF Band	S:S
Diplex Mode	Diplex
LNA[a] Selection	LNA-1
Telecom Link	DSS 14-Low Gain1-DSS 14
Telemetry Downlink Parameter Inputs	
Encoding	RS Concatenated with k=14, r=1/4 Convolutional Coding
Carrier Tracking	Suppressed
Oscillator	VCO
Sub-Carrier Mode	Squarewave
Carrier Loop Bandwidth, Hz	0.3000
Sub-Carrier Loop Bandwidth, Hz	0.0300
Symbol Loop Bandwidth, Hz	0.0300
Sub-Carrier Window Factor	0.25
Symbol Window Factor	0.60
Telemetry Usage	Suppressed Carrier Mode Phase 2
Telemetry Data Rate, bps	40
Telemetry Modulation Index, deg	90 (Step 55)
Telemetry Ranging Modulation Index, rad	0.00
Telemetry DOR Modulation Index, rad	0.00
Mission Phase	Cruise
DSN Site	Gold-Gold
DSN Elevation	In View
Weather/CD	25
Attitude Pointing	MZ Pointed
External Data	
Earth-Craft Range, km	7.3012×10^{8}
Earth-Craft Range, AU	4.8806
Jupiter-Craft Range, km	1.9062×10^{7}
Jupiter-Craft Range, AU	1.2742×10^{-1}
Sun-Earth-Craft Angl, deg	96.82
Sun-Craft-Earth Angle, deg	11.19
Jupiter-Earth-Craft Angl, deg	1.08
One-Way Light Time, hh:mm:ss	00:40:35
Station Elevation, deg	56.67
Degrees-off-Boresight: LGA1, deg	0.81
Clock: LGA1, deg	0.00
Added S/C Antenna Pointing Offset, deg	0.00
DSN Site Considered:	DSS-14/DSS-14
At Time:	0.00 hours after the start time

[a] Low-noise amplifier.

Table 5-3. Galileo downlink DCT (DSS-14, 60 bps telemetry) (cont'd).

Link Parameter	Design Value	Fav Tol	Adv Tol	Mean Value	Var
Transmitter Parameters					
1. S/C Transmitter Power, dBm	41.74	0.75	–1.61	41.45	0.2423
2. S/C Transmitter Circuit Loss, dB	–0.70	0.10	–0.10	–0.70	0.0033
3. S/C Antenna Gain, dBi	8.10	0.39	–0.40	8.10	0.0260
4. Degrees-off-Boresight Loss, dB	–0.00	0.39	–0.40	–0.01	0.0520
5. S/C Pointing Control Loss, dB	0.00	0.00	0.00	0.00	0.0000
6. EIRP (1+2+3+4+5), dBm	48.84	1.71	–1.71	48.84	0.3237
Path Parameters					
7. Space Loss, dB	–276.94	0.00	0.00	–276.94	0.0000
8. Atmospheric Attenuation, dB	–0.04	0.00	0.00	–0.04	0.0000
Receiver Parameters					
9. DSN Antenna Gain, dBi	63.34	0.10	–0.10	63.34	0.0017
10. DSN Antenna Pointing Loss, dB	–0.10	0.10	–0.10	–0.10	0.0033
11. Polarization Loss, dB	–0.02	0.10	–0.10	–0.02	0.0033
Total Power Summary					
12. Total Received Power (6+7+8+9+10+11), dBm	–164.91	–1.73	1.73	–164.91	0.3320
13. SNT at Zenith, K	17.65	–0.70	1.30	17.85	0.1717
14. SNT Due to Elevation, K	0.02	0.00	0.00	0.02	0.0000
15. SNT Due to Atmosphere, K	2.29	0.00	0.00	2.29	0.0000
16. SNT Due to Jupiter, K	0.00	0.00	0.00	0.00	0.0000
17. SNT Due to the Sun, K	0.00	0.00	0.00	0.00	0.0000
18. SNT Due to Galactic Background Noise, K	0.50	0.00	0.00	0.50	0.0000
19. Total SNT (13+14+15+16+17+18), K	20.46	–0.70	1.30	20.76	0.1111
20. Noise Spectral Density, dBm/Hz	–185.49	–0.15	0.27	–185.43	0.0049
21. Received P_t/N_0 (12–20) dB-Hz	20.52	1.74	–1.74	20.52	0.3369
22. Required P_t/N_0, dB-Hz	19.51	0.00	0.00	19.51	0.0000
23. P_t/N_0 Margin (21–22), dB	1.01	1.74	–1.74	1.01	0.3369
24. P_t/N_0 Margin Sigma, dB	0.00	0.00	0.00	0.58	0.0000
25. P_t/N_0 Margin–(2+NConf) Sigma (23–2×24), dB	–0.15	0.00	0.00	–0.15	0.0000
Carrier Performance					
26. Costas Loop SNR, dB	23.26	1.74	–1.74	23.26	0.3369
27. Costas Loop SNR Required, dB	17.00	0.00	0.00	17.00	0.0000
28. Costas Loop SNR Margin (26–27), dB	6.26	1.74	–1.74	6.26	0.3369
Telemetry Performance					
29. Telemetry Data Suppression, dB	0.00	0.00	0.00	0.00	0.0000
30. Ranging Data Suppression, dB	0.00	0.00	0.00	0.00	0.0000
31. DOR Data Suppression, dB	0.00	0.00	0.00	0.00	0.0000
32. Received P_d/N_0 (21+29+30+31), dB-Hz	20.52	1.74	–1.74	20.52	0.3369
33. 2-Sigma P_d/N_0 (32–2×sqrt(32var)), dB-Hz	19.36	0.00	0.00	19.36	0.0000
34. Data Rate, dB-Hz	16.02	0.00	0.00	17.78	0.0000
35. Available E_b/N_0 (32–34, dB	4.50	1.74	–1.74	4.50	0.3369
36. Loss Receiver (TPAP[a]), dB	–0.29	0.00	0.00	–0.29	0.0000
37. Loss Scintillation (TPAP), dB	0.00	0.00	0.00	0.00	0.0000
38. Loss FSR (TPAP), dB	–0.40	0.00	0.00	–0.40	0.0000
39. Loss Decoding (TPAP), dB	–0.40	0.00	0.00	–0.40	0.0000
40. Losses Total System (36+37+38+39), dB	–1.09	0.00	0.00	–1.09	0.0000

[a] Telecom prediction and analysis program.

Table 5-3. Galileo downlink DCT (DSS-14, 60 bps telemetry) (cont'd).

Link Parameter	Design Value	Fav Tol	Adv Tol	Mean Value	Var
41. Output E_b/N_0 (35+40), dB	3.41	1.74	–1.74	3.41	0.3369
42. Output E_s/N_0, dB	–2.61	–1.74	1.74	–2.61	0.3369
43. Required E_b/N_0, dB	0.56	0.00	0.00	0.56	0.0000
44. E_b/N_0 Margin (41–43), dB	2.85	1.74	–1.74	2.85	0.3369
45. E_b/N_0 Margin Sigma, dB	0.00	0.00	0.00	0.58	0.0000
46. E_b/N_0 Margin–2 Sigma (44–2×45), dB	0.00	0.00	0.00	1.69	0.0000

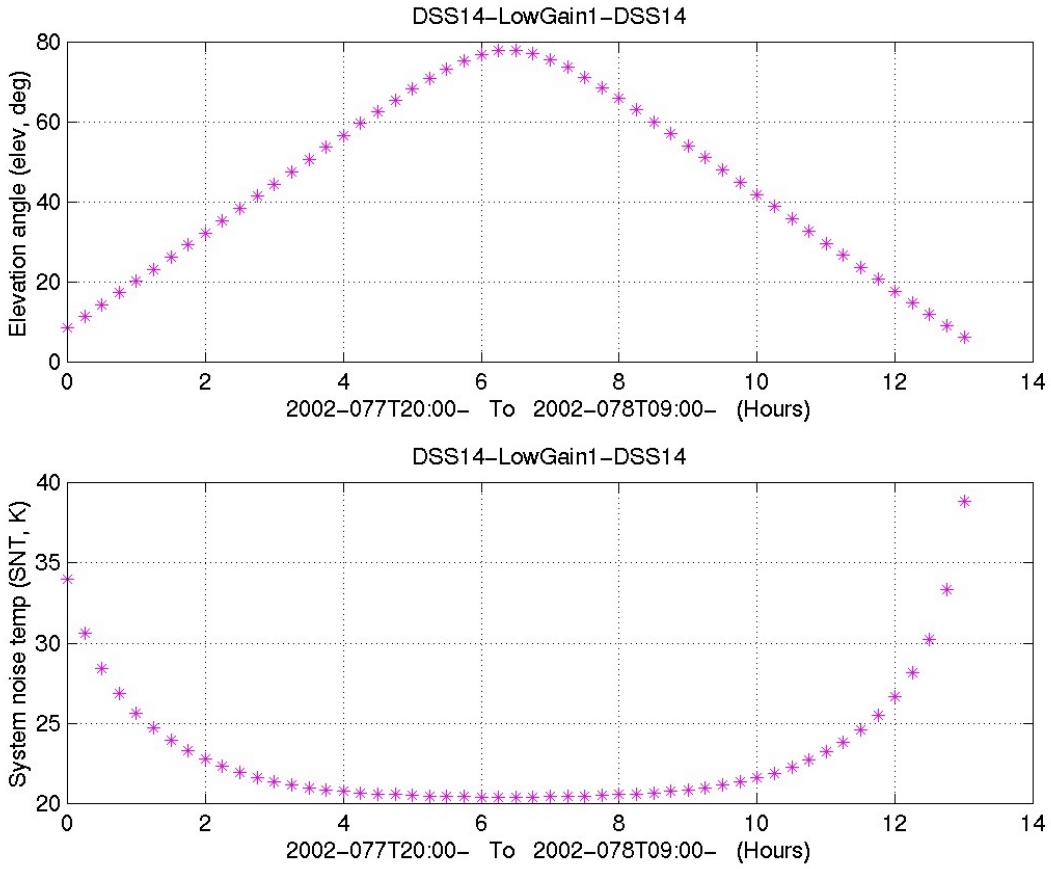

Fig. 5-1. DSS-14 elevation angle and system noise temperature on 2002-077.

5.2.1 Elevation Angle and SNT During a Single Pass

Figures 5-1, 5-2, and 5-3 cover a single DSS-14 station pass.

Because an uplink is required, DSS-14 is in the diplexed mode for this pass. The elevation angle at the time of the DCT (Fig. 5-1) is 56.7 deg, and the SNT is 20.5 K.

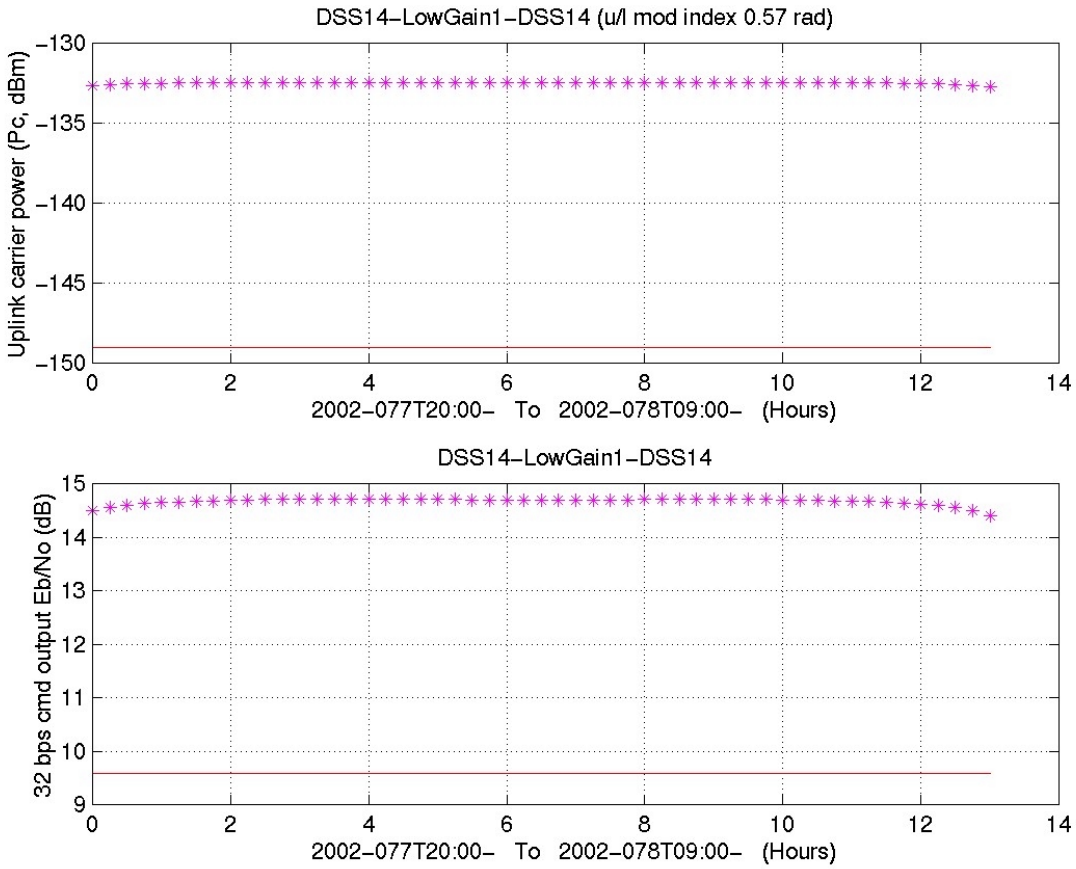

Fig. 5-2. Uplink performance from DSS-14 on DOY 2002-077.

5.2.2 Uplink Quantities During a Single Pass

The uplink P_c (top) and E_b/N_0 (bottom) in Fig. 5-2 each vary much less over the same range of elevation angle than the downlink P_c/N_0 and E_s/N_0 in Fig. 5-3, even though the S-band uplink and downlink are not that far apart in frequency.

As elevation angle changes, two uplink and three downlink values change. Variation of atmospheric attenuation and station antenna gain (affected by structural deformation) are similar on uplink and downlink. Station system noise temperature, the largest downlink contributor, is not a factor for uplinks.

Orbiter uplink P_c is in the engineering telemetry (in a channel called RFS AGC) from the spacecraft. As the figure shows, the threshold is –149 dBm. The value produced (–132.4 dBm at 00:00 UTC) assumes use of the 100-kW transmitter and a command modulation index of 0.57 rad. This index makes the P_c lower than the received total power of –130.9 dBm.

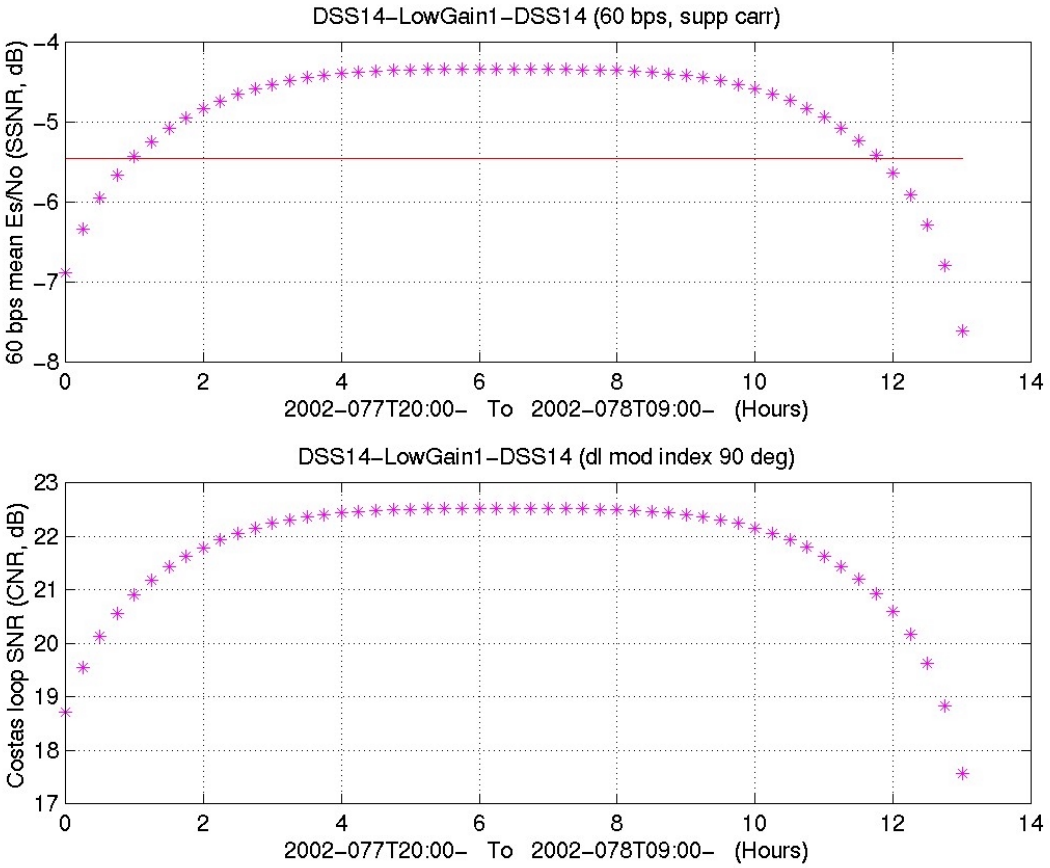

Fig. 5-3. Downlink performance at DSS-14 on DOY 2002-077.

5.2.3 Downlink Quantities During a Single Pass

The top plot of Fig. 5-3 shows the telemetry symbol SNR (E_s/N_0), and the bottom the carrier tracking loop SNR. The dominant quantity causing the variation is the station SNT shown in Fig. 5-1. Downlink quantities such as these vary considerably with elevation angle. The Galileo S-band mission uses a telemetry modulation index of 90 deg, producing a suppressed carrier downlink.

The station's BVR is configured with a Costas loop for receiving the suppressed carrier downlink. The Costas loop threshold SNR is 17 dB. The figure shows the achieved mean carrier SNR is higher than that for all elevation angles.

The mean E_s/N_0 for 60 bps telemetry is several dB below the –5.4 dB threshold at the low elevation angles near the beginning and end of the pass. The Table 5-3 DCT shows there is margin at the next lower data rate, 40 bps, at the lower elevation angles.

5.2.4 Range and One-Way Light Time During GEM and GMM

Figures 5-4 through 5-7 display long-term Galileo link capability, assuming DSS-14 is at a constant elevation angle of 25 deg, with a data point plotted once every 20 days. The time scale is in weeks starting from DOY 1997-342 and continuing to DOY 2002-078.

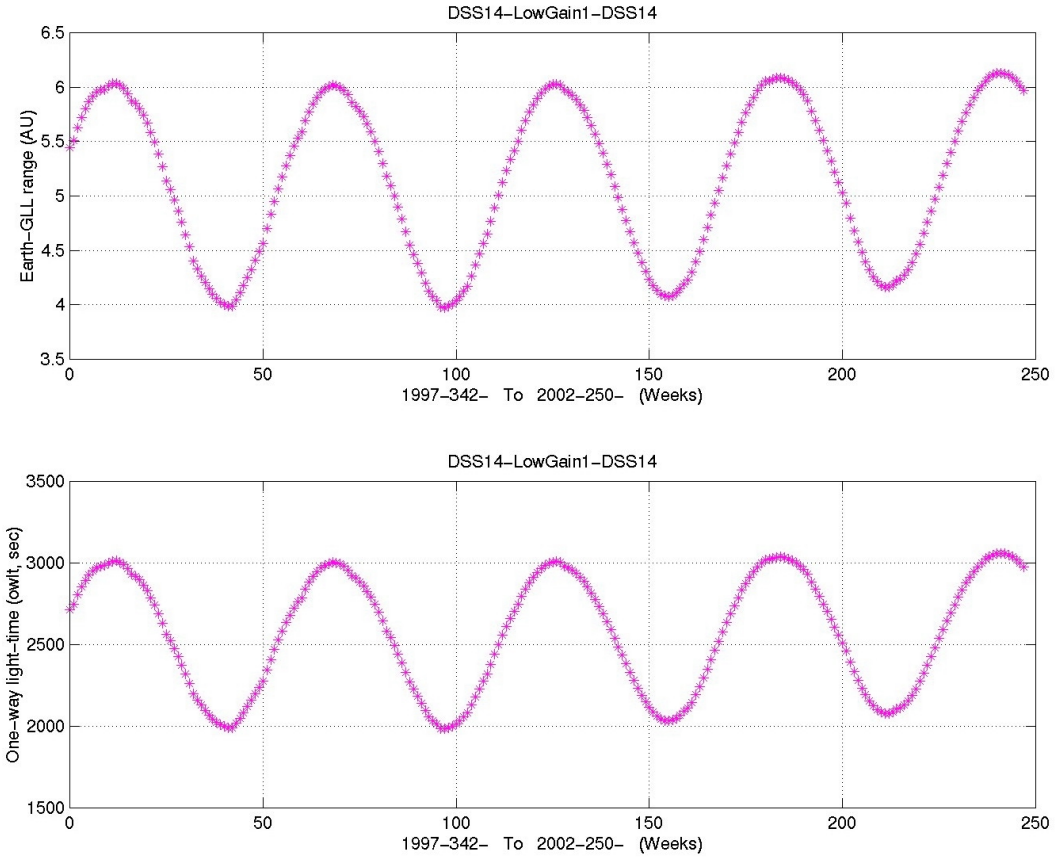

Fig. 5-4. Range and OWLT from DSS-14 to Galileo in GEM and GMM.

Galileo is in orbit around Jupiter. With a negligibly small error in the resulting performance in dB, the spacecraft-Earth range, top plot, is nearly the same as the Jupiter-Earth range. As the plot shows, the range varies from just greater than 4 AU to just greater than 6 AU with a periodicity of about 13 months as the planets move in the orbits about the Sun. The difference in performance is proportional to $20\times\log(\text{range}_{max}/\text{range}_{min})$, or about 3.6 dB.

The one-way light time (OWLT), Fig. 5-4, is proportional to the station-spacecraft range.

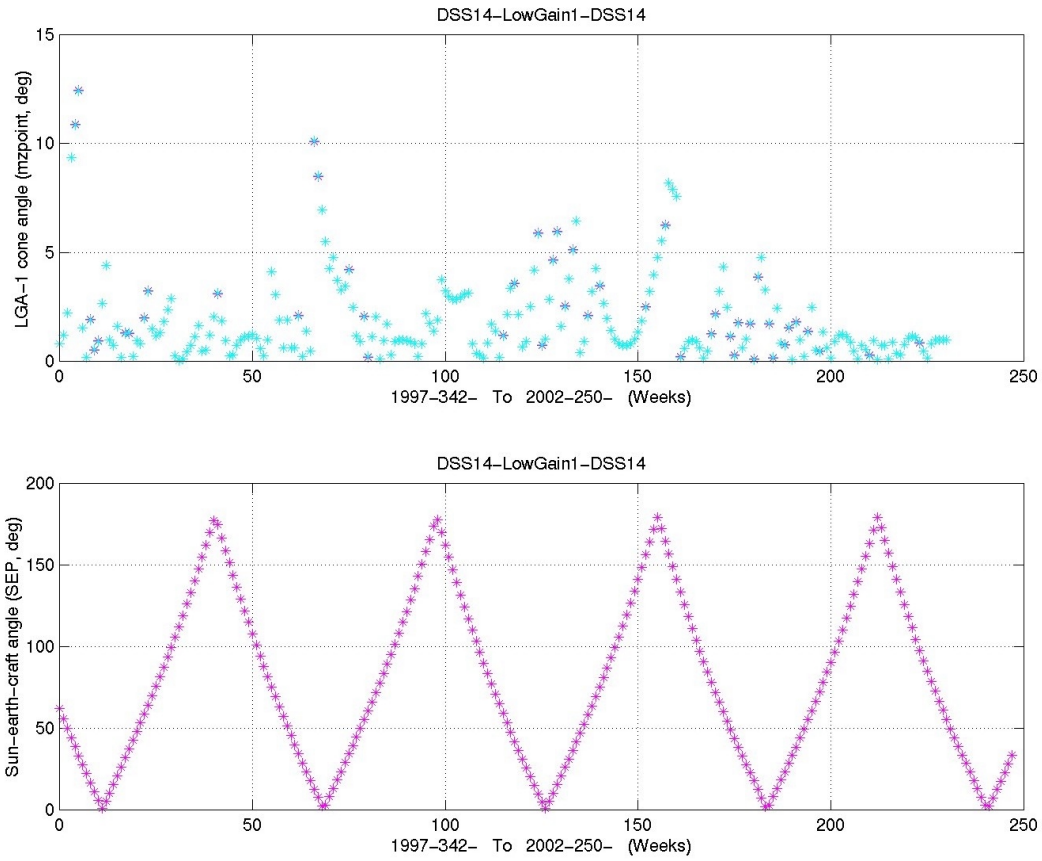

Fig. 5-5. LGA-1 pointing angle and Sun-Earth-craft angle in GEM and GMM.

5.2.5 LGA-1 Boresight Angle and Sun-Earth-Craft Angle During GEM and GMM

The angle from the LGA-1 boresight to the station (top plot) depends on the size and timing of spacecraft turns that keep the antenna oriented. The name MZPOINT refers to the orbiter's –Z axis (LGA-1 boresight). The project goal is to keep the angle smaller than 4 deg to minimize downlink performance losses. However, this requires attitude reference stars available to the AACS at the desired inertial attitudes. The larger angles shown in the plot result from lack of suitable stars at the times turns would be made to keep the angle smaller.

The Sun-Earth-craft (SEC) angle[2] (bottom plot) is the driving factor in solar conjunction planning, as described in Section 6.7. Conjunctions occur about every 13 months, when the angle is small. Modulation index and bandwidth reconfiguration are made for SEC angles smaller than 22 deg, and commanding is prohibited for angles smaller than 7 deg.

[2] In other articles of the Design and Performance Summary series, this angle is called the Sun-Earth-probe (SEP) angle, its traditional name at JPL. Because the Galileo mission includes a probe spacecraft, the term SEC angle is used in the Galileo article. The SEC angle most commonly is used in planning solar conjunction communications.

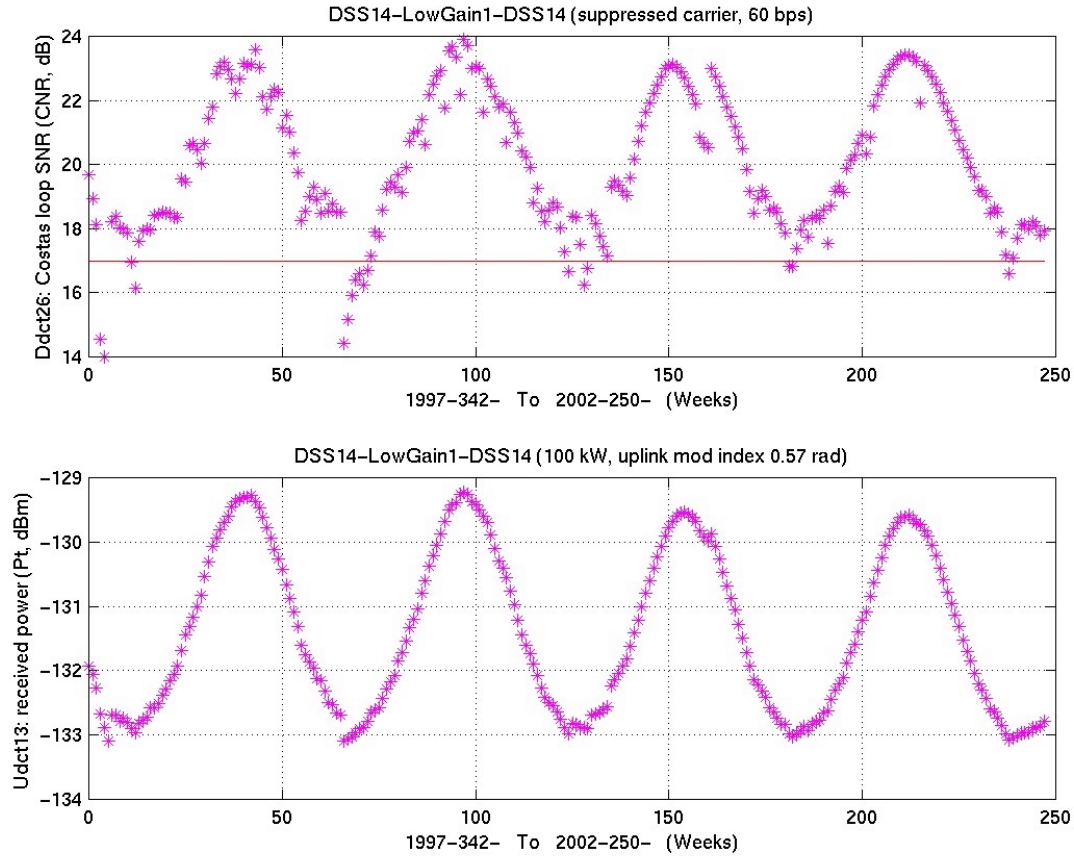

Fig. 5-6. Uplink and downlink carrier performance in GEM and GMM.

5.2.6 Downlink and Uplink Carrier Performance During GEM and GMM

The Costas loop SNR (top plot) remains above the 17 dB threshold except when the range is near maximum and the MZPOINT angle is larger than usual. Additional variation would be apparent if the full range of station elevation angles were shown rather than only 25 deg Nor are the additional degradation effects of solar conjunction modeled in this plot.

The uplink received power (bottom plot) shows somewhat less variation because the LGA-1 pattern is somewhat broader at the uplink frequency. Also the carrier SNR is nonlinear with total received downlink power, indicating greater carrier tracking difficulty at low levels.

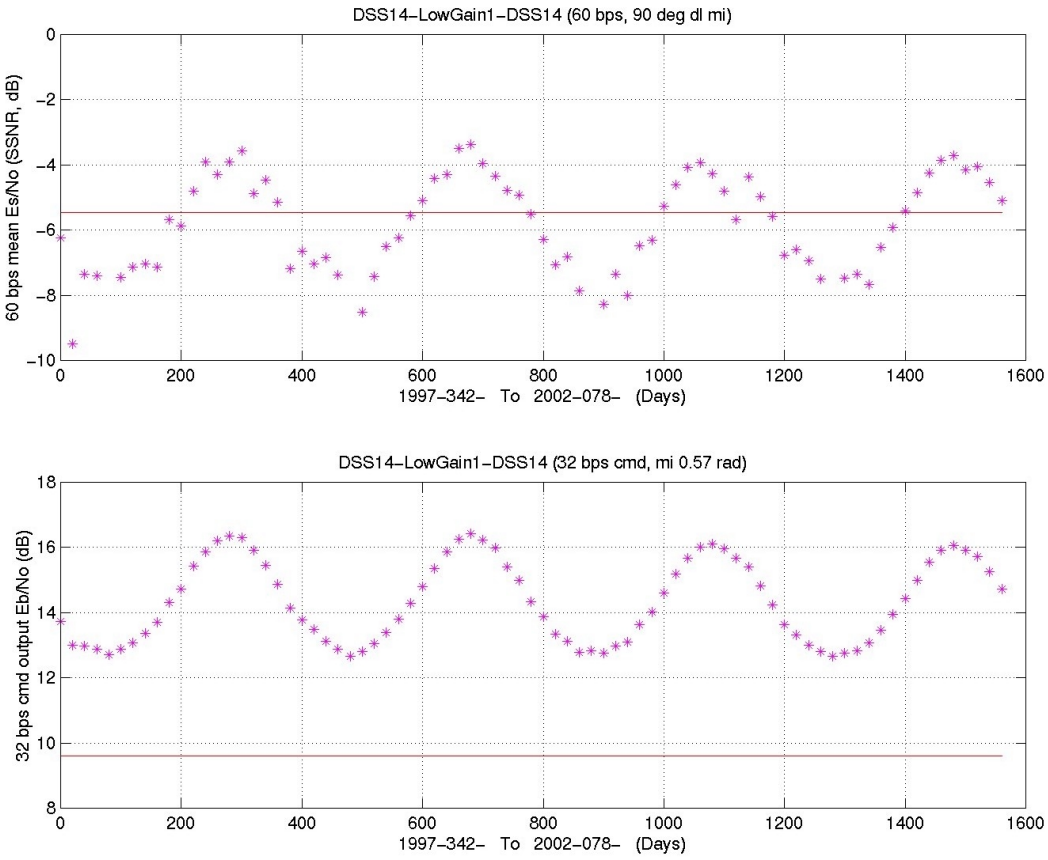

Fig. 5-7. Uplink command and downlink telemetry performance in GEM and GMM.

5.2.7 Telemetry and Command Performance During GEM and GMM

The telemetry E_s/N_0 (top plot) mimics the downlink carrier performance in Fig. 5-6, and the command E_b/N_0 (bottom plot) mimics that of the uplink carrier power.

For (14,1/4) coding, the telemetry threshold of +0.6 dB E_b/N_0 is –5.4 dB referenced to E_s/N_0. The plot shows that the 60-bps rate can be supported at 25-deg elevation at the smaller ranges. Using a non-diplexed mode, or the DSS-43 ultracone, results in the availability of 80 and 120 bps at smaller ranges. At larger ranges, rates down to 8 bps are required, especially inside the 22-deg SEC angle conjunction limit.

The command E_b/N_0 shows that 32-bps command capability is never a problem for a 100-kW transmitter. Because solar noise is not Gaussian, commanding is not scheduled inside 7-deg SEC angle. When commanding inside the 7-deg limit was occasionally required because of a ground or spacecraft problem, use of the full 400-kW power capability and multiple transmissions were successful (to about 4-deg SEC angle, the smallest angle attempted).

Section 6

Telecom Operational Scenarios

6.1 Planned and Actual DSN Coverage

The pre-launch plan was for Galileo to use primarily a set of three 34-m stations, one each at Goldstone, Canberra and Madrid. Communications assumed the use of the orbiter's HGA* (for S-band uplink and X-band downlink) when the HGA could be Earth-pointed and one of the LGAs (for S-band uplink and downlink) during maneuvers or at other times the HGA couldn't be Earth-pointed. The 34-m tracking station at Weilheim, operated by GSOC was an integral part of the planned cruise mission.

Upon failure of the HGA to deploy in 1991, the project converted the station coverage plan for most of the remaining four years of the interplanetary cruise to the 70-m net only, with S-band uplink and S-band downlink via the LGA.

In addition, with the S-band mission in place for a substantial portion of the prime orbital mission, the DSN was operated in an arrayed configuration for Galileo passes. Both intra-site and inter-site (intercontinental) arraying was used, to increase the effective receiving antenna aperture and therefore the supportable downlink rate. This arraying involved real-time combining of the spacecraft signals from the DSN 70-m and 34-m antennas at Canberra with those from the 70-m and 34-m antenna at Goldstone. The combined signals were enhanced further by the addition of the signal from the Australian 64-m radio astronomy antenna at Parkes. The array gain, relative to a single 70-m station, varied from about 1 dB (one 70-m station with one 34-m station) to almost 4 dB (full array, including Parkes).

* Look up this and other abbreviations and acronyms in the list that begins on page 63.

6.2 Launch Phase

The Space Shuttle Atlantis, on Mission STS-34, launched the Galileo spacecraft (the orbiter and the attached probe) on October 18, 1989[1] [21].

Prior to the separation of the spacecraft and the attached Inertial Upper Stage (IUS) from the shuttle, communications for most activities on STS-34 were to be conducted through the TDRSS, a constellation of three communications satellites in geosynchronous orbit 35,900 km above the Earth. A minimum amount of IUS/spacecraft telemetry data was sent via the shuttle downlink. During the first minutes of flight, three NASA Spaceflight Tracking and Data Network (STDN) ground stations received the downlink from the shuttle. Afterwards, the TDRS-East and TDRS-West satellites provided communications with the shuttle during 85 percent or better of each orbit.

The spacecraft/IUS were deployed from the shuttle about 6 hours into flight. The Galileo orbiter's receiver and command detector had remained on through launch. Command "discretes" from the IUS activated the orbiter command and data subsystem (CDS) commands to select the LGA (LGA-1), turn the S-band exciter on, and then turn the S-band TWTA on in the low-power mode. After a 5-minute TWTA warm-up, the orbiter telecom system was ready to support the first independent downlink from the orbiter: 1200 bps engineering data in the "TDRS mode" (no subcarrier, direct carrier modulation at 90 degs modulation index).

Prior to the first DSN acquisition, the CDS commanded the TMU to the "DSN mode" which has been used for the rest of the mission. The 1200 bps rate continued, but now on the 22.5- kHz subcarrier and with a different modulation index.[2] The CDS also commanded the RFS to the TWNC off mode, so the downlink carrier could provide two-way Doppler data for initial trajectory determination.

Approximately 9 hours after the orbiter separation from the IUS, the CDS stored sequence switched the data rate from 1200 bps to 28.8 kbps, on the 360-kHz subcarrier and with a modulation index change. The launch-phase spacecraft data from the orbiter tape recorder was played back at this rate. Following playback, routine real-time engineering telemetry resumed at the 1200 bps rate.

6.3 Cruise Phase

The "VEEGA" (Venus-Earth-Earth gravity assist) cruise to Jupiter included a flyby of Venus about 90 days after launch, followed by two flybys of Earth.[3] Following the second flyby

---

[1] Originally the Galileo science mission was planned and the orbiter and probe spacecraft designed for a 1982 launch. Changes in launch vehicle and the Space Shuttle Challenger accident delayed Galileo's launch from 1982 to 1986 to 1989. The redesign for a 1986 launch put the spacecraft in the shuttle bay with a Centaur booster capable of a direct launch to Jupiter. The post–Challenger redesign for the eventual 1989 launch required replacing the powerful, Lox/LH2-burning Centaur with the weaker, but safer SRM (solid rocket motor) IUS and longer, complex, gravity-assisted trajectory.

[2] The orbiter, like other JPL missions tracked by the DSN, has a specific subcarrier frequency and modulation index setting for each data rate. During the first DSN pass, rates of 1200 bps and 28.8 kbps were planned. These rates are associated with 22.5-kHz and 360-kHz subcarrier frequency, and with 68-deg and 80-deg modulation index, respectively.

[3] The change to a 1989 shuttle launch also required redesign of the interplanetary cruise trajectory to include a flyby of Venus (and the two of Earth) for enough energy to reach Jupiter. Flying inward toward the Sun resulted in the need for redesign of the spacecraft's thermal control and the addition of LGA-2 to maintain communications with Earth on the Venus leg. See http://www.jpl.nasa.gov:80/galileo/mission/journey-cruise.html for more information on the cruise phase.

of Earth, the spacecraft passed the orbit of Mars and went through the asteroid belt, the orbiter finally reaching Jupiter December 7, 1995. Release of the probe from the orbiter was in July 1995, with the probe entering Jupiter's atmosphere on the same day as the orbiter went into orbit around Jupiter [22].

The Venus flyby occurred on February 10, 1990 at an altitude of 16,000 km, with data playback scheduled the following October when the spacecraft would be closer to the Earth. The orbiter was originally designed thermally for operation only between Earth and Jupiter, where sunlight is 25 times weaker than at Earth and temperatures are much lower. The VEEGA mission exposed the spacecraft to a hotter environment in the region between Earth and Venus. Engineers devised sunshades to protect the craft. For the shades to work, the –Z axis must be aimed precisely at the Sun, with the HGA remaining furled for protection from the Sun's rays until after the first Earth flyby. The original plan was to deploy and begin using the HGA within 2 months of launch. The VEEGA mission necessitated a wait until the spacecraft was close to Earth to receive a high volume of recorded Venus data at rates up to 134.4 kbps, transmitted through the LGA.

The first Earth flyby (Earth-1) occurred on December 8, 1990 at an altitude of 960 km and the second on December 8, 1992 at an altitude of 305 km. Between the two Earth flybys was a flyby of the asteroid Gaspra on October 29 1991. On the flight to Jupiter was a flyby of the asteroid Ida in August 28, 1993. The Gaspra flyby altitude was 1,600 km at a flyby velocity of about 30,000 km/hr. The Ida flyby altitude was about 2,400 km at a velocity of nearly 45,000 km/hr relative to Ida. The second Earth flyby included an optical communications experiment: the detection in the SSI of laser pulses transmitted via a telescope at Table Mountain, California [4]. The experiment yielded good data in support of theoretical studies and encouraged the further development of the technology for optical communications.

Within a few days of launch, the S-band TWTA was switched to its high power mode, where it has generally remained since. During cruise, the orbiter communicated via either the primary LGA-1 or the aft-facing LGA-2. LGA-1 is boresighted in the same direction as the HGA. LGA-2 was added to the spacecraft when the mission was redesigned to include a Venus flyby. Because of the flyby geometry relative to the tracking stations, LGA-2 was also required for about two days at Earth-1 and could have been used for a similar period at Earth-2. The project's antenna selection tradeoff during planning for Earth-2 was reduction in risk (two fewer antenna switches) at a small cost in decreased communications capability.

Cruise telemetry data rates were either 1200 bps or 40 bps, using the (7,1/2) convolutional code. The lower rate was always required for trajectory correction maneuvers at large LGA offpoint angles from Earth and at the larger Earth-spacecraft ranges. The single Galileo command rate is 32 bps, uncoded. When more command link performance was required, this was achieved by use of the high power (100 kW) transmitters at the 70 stations. During the early portion of cruise, turnaround ranging was possible via the LGA. Around the time of Earth-1, the delta-DOR tones were also transmitted on the S-band downlink carrier [23] and used to verify the navigation solution for the Earth-1 flyby.

The Galileo probe was turned on and tested, using the S-band orbiter-DSN links, during cruise.

6.4 HGA Deployment Attempts

The orbiter HGA is a very close derivative of the unfurlable TDRS antennas and was built for Galileo by the same manufacturer. The 4.8-m parabolic reflector is gold-plated molybdenum wire mesh attached to 18 graphite epoxy ribs. Each rib rotates about a pivot at the base. A

ballscrew on the centerline, driven by redundant motors, raises a carrier ring attached to the ballnut. A pushrod connects each rib to the carrier. As the carrier rises, the ribs were intended nominally to rotate symmetrically into position [24].

The HGA deployment phase began when the temperature control constraints permitted Earth-pointing of the HGA. On April 11, 1991, the orbiter began to deploy the HGA under computer-sequence control [25]. The antenna had been furled and protected behind a small sunshade for almost 18 months since launch, in which the spacecraft spent a time closer to the Sun than to the Earth. Communications, including Venus and Earth-moon science data return, had been using the LGAs.

Within minutes, Galileo's flight team, watching spacecraft telemetry from 37 million miles away, could see that something was wrong: The deployment motors had stalled, something had stuck, and the antenna had opened only part way.

Within weeks, a "tiger team" had thoroughly analyzed the telemetry, begun ground testing and analysis, and presented its first report. They attributed the problem to the sticking of a few antenna ribs due to friction between their standoff pins and their sockets. The first remedial action was taken—turning the spacecraft to warm and expand the central tower, in hopes of freeing the stuck pins.

A special HGA Deploy Anomaly Review Board, mostly made up of experts from outside JPL, met with the project and its tiger team monthly. In June 1992, a comprehensive two-day workshop was held at JPL, attended by nearly fifty technical specialists from outside JPL, reviewing the work to date and seeking new ideas [26].

Beyond thermal cycling, the tiger team developed other ideas to loosen the stuck ribs. These ideas, generally seconded by the review board and workshop experts, included producing a small vibration and shock by retracting the second low-gain antenna (on a pivoting boom), pulsing the antenna motors, and increasing the spacecraft spin rate to a maximum of 10 rpm (normally about 3 rpm). The deploy motor pulsing was called "hammering." On December 28, 1992, a warming turn produced maximum tower extension from thermal expansion, but no rib released. The next day over 2,000 pulses were applied. The ballscrew rotated about 1.5 turns (about the amount predicted after ground tests of the spare HGA at JPL) before stalling again after a few hundred pulses. Eventually over 13,000 hammer pulses were applied through January 19, 1993 [27].

To see if the partly deployed antenna was of any use for communications, the flight team operated the X-band TWTA downlink and the XSDC X-band uplink through the HGA to assess link capability in the stuck position. Although the orbiter received the X-band uplink and the DSN received the X-band downlink, the downlink capability was only slightly greater than available at S-band through the LGA. The project considered the sequencing complexity to maintain HGA pointing to Earth as too risky in trade for a small improvement.

A two-year campaign to try to free the stuck ribs, including seven heating or cooling cycles, failed to release any more ribs. The project concluded there was no longer any significant prospect of deploying the HGA. One last attempt was made in March of 1996.[4] When that also was unsuccessful the Project continued to devote its resources to completing the implementation of the S-band mission, using only LGA-1.

[4] See http://www.jpl.nasa.gov/galileo/faqhga.html for more discussion of the HGA and the attempts to unstick it.

6.5 Probe Separation, Jupiter Cruise, and Jupiter Orbit Insertion

This Jupiter cruise phase began four months and ended two months before Jupiter encounter. In addition to the actual separation of the probe from the orbiter on July 13, 1995, this phase included probe turn-on and final checkout as well as the preliminary positioning of the orbiter-mounted relay radio hardware (RRH) antenna. This articulated antenna was repositioned several times during probe descent.

The orbiter's tape recorder malfunctioned October 11, less than two months before JOI. The tape recorder failed to stop rewinding as expected after recording some imaging data. Commands were sent to halt the tape recorder immediately upon discovery of the problem, but by that time it had been trying to rewind with the tape stuck in one position for 15 hours. The flight team investigated the problem using an identical recorder on the ground. They also began redesigning the encounter sequence in case the recorder could not be used again. Within a week, the project had a plan to return all of the planned probe relay data as well as 50% of orbiter science data planned for the S-band mission, even without the tape recorder. On October 20, the recorder was tested and proved to be still operational. Though the recorder was considered to be unreliable under some operating conditions, the ground tests showed the problem to be manageable. Periodic "tape conditioning" sequences to avoid further tape sticks were instituted, and the recorder continued to work through the prime and extended missions.[5]

The JOI and probe relay phase was the most complex and scrutinized phase of the mission.[6] This mission phase began two months before JOI and ended a month after JOI. Activities included 2 approach trim maneuvers, a close flyby of the Jovian satellite Io, probe entry and data relay, JOI, and a post-JOI orbit trim maneuver. The orbiter passed through the most intense radiation environment of the prime mission[7] during the Io flyby at a distance of 4Rj (Jupiter radii). About two hours after the first signal was received from the probe, the orbiter's 400-Newton main engine fired for 49 minutes to achieve JOI. For telecom, the Doppler variation through the closest-approach station pass was several times the amount observed in interplanetary cruise or orbital cruise passes.

Continuous DSN coverage was required throughout this phase for navigation and telemetry. Unique coordination with the DSN was required to ensure the proper sequence of bandwidth settings in the station's Block 5 receiver. Also, unique uplink acquisition and tuning profiles were coordinated to minimize the Doppler variation through the close encounter pass. Additional telecom factors included planned loss of downlink at the end of JOI (due to Doppler) and a solar conjunction with loss of data expected about one week after JOI. Within these constraints, the orbiter and ground telecom systems were configured for the maximum supportable downlink data rate via the LGA, with probe data being the highest priority.

---

[5] The flight team most recently restored the recorder's capability in mid-2002. During a standard tape conditioning activity on April 12, 2002, fault protection in the flight software's tape manager tripped, locking out subsequent tape commands. This type of fault trip is caused by a failure of the tape rate to properly synchronize with an internal timing reference. On May 7, a test confirmed that the recorder's motor was operating as expected and that the motor current was consistent with the tape being stuck to one or more heads. On June 8, the tape recorder was successfully unstuck during a high rate slew. The tape pulled free shortly after the slew command was issued and behaved normally during a subsequent short playback slew. Over the next several weeks a series of tape motions to condition the tape and reduce the possibility of future hard sticks was begun. Ground tests combined with a revised empirical model are being used to define future tape operating strategies [28].

[6] Section 7 describes the requirements, implementation, and performance of the probe-to-orbiter relay link.

[7] There have been six subsequent Io flybys in GEM and GMM, and an even more intense radiation environment is expected around the Amalthea flyby in November 2002.

Section 7 describes the probe-orbiter relay system and links in some detail. In summary, the probe returned data through the RRH for about one hour. The radio signal from the probe ended 61.4 minutes into the entry when the high atmospheric temperatures caused the probe's radio transmitter to fail [29]. For a "first look" of probe data, the orbiter transmitted from CDS memory the highest-priority 40 minutes of probe data by December 13. The orbit plan also included multiple playbacks of all probe data from the tape recorder. The playback campaign began on January 3, 1996 (after solar conjunction) and ended April 15 after three full or partial playbacks.

6.6 Orbital Operational Phase

The orbiter's prime mission included 11 orbits of Jupiter, with flybys of one or more Jovian satellites on 10 of these encounters.[8] The prime mission was defined to end December 7, 1997 (two years after JOI), at which time the GEM began. The GEM ended December 7, 1999, at which time the GMM began. That mission continues into 2003.

As defined by the flight software, two major downlink spacecraft telecom configurations existed during the prime mission, "Phase-1" and "Phase-2" [6]. Phase-1 downlinked the same TDM data that had been used through cruise. The TDM telemetry data was (7,1/2) convolutionally coded, modulating the 22.5 kHz subcarrier, and with the subcarrier modulating the carrier in a residual carrier mode (modulation index 72 deg maximum). The S-band TWTA operated in its high-power mode. LGA-1 was kept pointed as close to Earth as possible. On the ground the link was supported with the BVR.

Phase-2, which became operational in June 1996, involved significant reprogramming of the CDS to produce a packet-formatted telemetry stream, to partially code the stream for input to the TMU, and to set a data rate at one of a small set of rates between 8 bps and 160 bps (the TMU and RFS are not reprogrammable in flight). The Phase-2 downlink used a concatenation of block-length 255 Reed-Solomon coding, interleaved to a depth of 8, and (14,1/4) convolutional encoding. The packet-mode symbol stream modulated the 22.5 kHz subcarrier as in Phase-1, but the subcarrier modulated the carrier at a 90 deg modulation index, producing a suppressed carrier.

In support of Phase-2, the ground system implemented the full spectrum recorder/full spectrum combiner (FSR/FSC), the buffered telemetry demodulator (BTD) and the feedback concatenated decoder (FCD). The FSR/FSC enabled the use of efficient local and intercontinental station-arraying with signal-combining at IF (intermediate frequency). For redundancy, the station operated with two FCDs, the second one receiving demodulated channel symbols from a BVR. The BVR also produced two-way Doppler for navigation.

To maximize the downlink "bits-to-ground" data volume return per pass, orbiter sequencing system software was upgraded to incorporate the data-rate capability file (DRCF) prediction into an automated telemetry-rate generator (TLMGEN) to create the series of commands to change the downlink rate in coordination with the downlink configuration and allocated station passes. Routinely, the rate would be set so that that residual (defined as the actual achieved symbol SNR minus the predicted symbol SNR) remained in the 0.5- to 1-dB range. The DRCF/TLMGEN rate accounted for diplexed vs. low-noise configuration of the station, the changing elevation angle, and the particular stations that were assigned to the array at a given time. It also sequenced "fill data" (defined as that which could be lost without penalty) at

[8] The fifth encounter, in January 1997, occurred during a solar conjunction. No satellite close-approach was planned, and this phasing orbit for subsequent encounters, was sometimes referred to J5 for Jupiter 5.

times the downlink was likely to be out of lock due to a one-way to two-way transition or other defined spacecraft conditions such as turns for trajectory correction maneuvers.

The telecom analyst maintained plots of residual (observed minus predicted) values of symbol SNR and SNT for representative data rates during each 70-m station pass. Individual data plots could be displayed by such criteria as station ID or diplexer mode. This allowed the project to determine if one station or one operating mode became degraded relative to others. By superimposing a plot of LGA off-Earth angle, for example one like the top portion of Fig. 5-5 on the residuals, it was possible to assess the quality of the pre-launch antenna pattern modeled in the prediction software. During the prime mission, the pattern was updated for the DRCF/TLMGEN software.

6.7 Solar Conjunction

Solar conjunction is difficult for communications because the radio signals traveling between the Earth and Jupiter pass through regions of high and variable charged-particle density close to the Sun.[9] Based on the observed Phase-2 performance in the latter half of 1996 and the experience gained in receiving the Phase-1 downlink in December 1995–January 1996, the telecom analysts devised a strategy to configure the links for the January–February 1997 conjunction. The strategy involved a succession of steps going in to the smallest SEC angle, then reversing these coming back out: (a) changing from suppressed carrier to residual carrier downlink mode, (b) reducing the telemetry modulation index, (c) reducing the data rate, and (d) increasing the carrier-loop bandwidth to larger than normal values.

The purpose for each of these changes is as follows:

- A suppressed carrier waveform requires a Costas loop for carrier tracking; the Costas loop is significantly more susceptible than a normal phase-locked loop to half-cycle slips resulting from the solar disturbances to signal amplitude and phase
- Reducing the telemetry modulation index puts more of the power into the carrier, increasing the ability of the carrier-tracking loop to hold lock
- Reducing the data rate makes up for the reduced amount of power available in the data sidebands relative to the carrier
- Increasing the carrier-loop bandwidth (CLBW) reduces the loop SNRs, but permits the loop to remain in lock through a wider spectrum of (non-Gaussian) solar fluctuations.

The same strategy has successfully been used for subsequent conjunctions, which occur every 13 months. The configuration changes are based solely on the SEC angle. Independent of the solar cycle or short-term solar fluctuations, the size of the SEC angle proves to be the single best predictor of solar effects on Galileo S-band communications. The following specific strategy was first used in 1997 and has worked well for each conjunction subsequently:

[9] A superior solar conjunction (like Galileo's) occurs when the Sun is between the spacecraft and the Earth. Planning for superior conjunction effects on deep-space links at JPL currently takes into account only the carrier-frequency band and the SEC angle. Solar activity varies in cycles, with the 11-year solar cycle near a maximum in 2000–2001. The effects on a link, caused by charged particles from the Sun producing amplitude and phase scintillation, may also be highly variable over periods of a few minutes to a few hours. Coronal-mass ejections (CMEs) of charged particles that cross the ray path between Earth and the spacecraft sometimes degrade Galileo S-band links even when the SEP angle is greater than 90 deg.

- At 22 deg SEC angle inbound (decreasing SEC angles), transition from the standard loop bandwidth mode (0.3 Hz CLBW) to 0.4 Hz CLBW. Conversely, outbound from conjunction at approximately 22 deg SEC, return to the standard mode
- At 18 deg SEC angle, transition from suppressed carrier mode (90 deg modulation index) to a residual carrier mode (60 deg modulation index) and a still wider CLBW of 0.6 Hz
- At 12 deg SEC angle, raise the data rate thresholds used for DRCF/TLMGEN downlink sequencing
- At 9 deg SEC angle, transition to a lower modulation index residual carrier mode and a wider bandwidth (51 deg mod index, 0.8 Hz CLBW)
- Within 7 deg SEC angle, impose a "moratorium" on commanding. Because of this constraint, all planned commanding, including resetting of the command loss timer, occurs outside 7 deg SEC
- Within 6 deg SEC angle, expect significant loss of telemetry data. Because of this expectation, the project elects to place only lower-value "fill data" on the downlink during the time the SEC angle is within 6 deg.

6.8 Galileo Europa Mission and Galileo Millennium Mission

These extended mission segments span the periods of December 1996–December 1998 and December 1998–September 2003, respectively. GEM encounters began with Europa-12 and ended with Io-25. The GMM encounters commenced with Europa-26 and are planned through Amalthea-34, followed by a final plunge into Jupiter's atmosphere [22]. The Io-24 and Io-25 flybys again subjected the spacecraft to the more intense regions of the Jovian radiation belts. Patches to the flight software had been made to minimize the effects of radiation-induced power-on reset flags that had halted some of the previous encounter sequences.

The same Phase-2 telecom mode that began in 1996 during the prime mission was continued through GEM and GMM except that station arraying was no longer scheduled. All uplink and downlink was scheduled through 70-m standalone passes. With reduced staffing in the telecom analysis area, routine generation of residual data has stopped. However, predictions for every station pass continue to be made. These are used to generate as-needed performance analysis for passes in which telemetry data is lost for "reasons unknown" or "low link performance."

Section 7

Probe-to-Orbiter Relay-Link Design

7.1 Overview

During interplanetary cruise, four in-flight probe checkout tests took place as the orbiter and probe traveled together.[1] Separation of the probe from the orbiter was completed on July 12, 1995. On December 7, 1995, both spacecraft arrived at Jupiter. As the probe entered Jupiter's atmosphere, the orbiter flew past Jupiter's satellite Io, received the relay data from the probe, and fired its main engine for orbit insertion around Jupiter.

The strategy for returning the probe data to Earth took into account several factors. The loss of the use of the orbiter HGA[*] prevented the downlink of real-time probe data during the encounter, leaving the orbiter's tape recorder to collect the data. To restore the redundancy implied by both real-time transmission and later playback of the probe data, a method was devised to store a reduced set of probe symbols in the spacecraft memory. Also, the frequency data (to detect Doppler shifts resulting from wind) from the probe receiver onboard the orbiter was stored in orbiter memory. An anomaly with the orbiter tape recorder on October 11, 1995 resulted in more tweaks to the strategy to minimize the risk of loss of probe data from the orbiter before it could be returned to Earth. Finally, because solar conjunction would cut communications from the orbiter to the Earth about a week after arrival, the strategy included playing back only the highest priority symbol set before conjunction, leaving the remaining playback until after conjunction, in January 1996.

7.2 Relay-Link Requirements and Design

Fig. 7-1 is a block diagram of the probe-to-orbiter relay link [30], with the bottom showing elements housed in the probe and the top showing those in the orbiter.[2] The probe instruments

[1] This probe operations overview and relay link performance summary sections come from [29].

[*] Look up this and other abbreviations and acronyms in the list that begins on page 63.

[2] The probe relay link requirements come from [30] and [31].

and flight software created two data streams called “A-string” and “B-string.” These represent two separate RF channels that are differentiated only by frequency and circular polarization sense. Each channel carried identical symbols, had a data rate of 128 bps, and was coded with a (7,1/2) convolutional code. The streams of symbols biphase modulated L-band carriers at 1387.0 and 1387.1 MHz in separate exciters.

A stable oscillator provided a 23-MHz frequency reference for the 1387.0 MHz carrier, and a (less stable) temperature-compensated crystal oscillator for the 1387.1 MHz carrier. The stable oscillator used a quartz crystal frequency source and was housed within a double-proportioned control oven. The 23-MHz oscillator outputs were frequency multiplied to the final carrier frequencies. The 1387.0 carrier has the stability required for radio science, the stability being in the range of 10^{-10} (due to pressure variations) to 10^{-9} (due to motion).

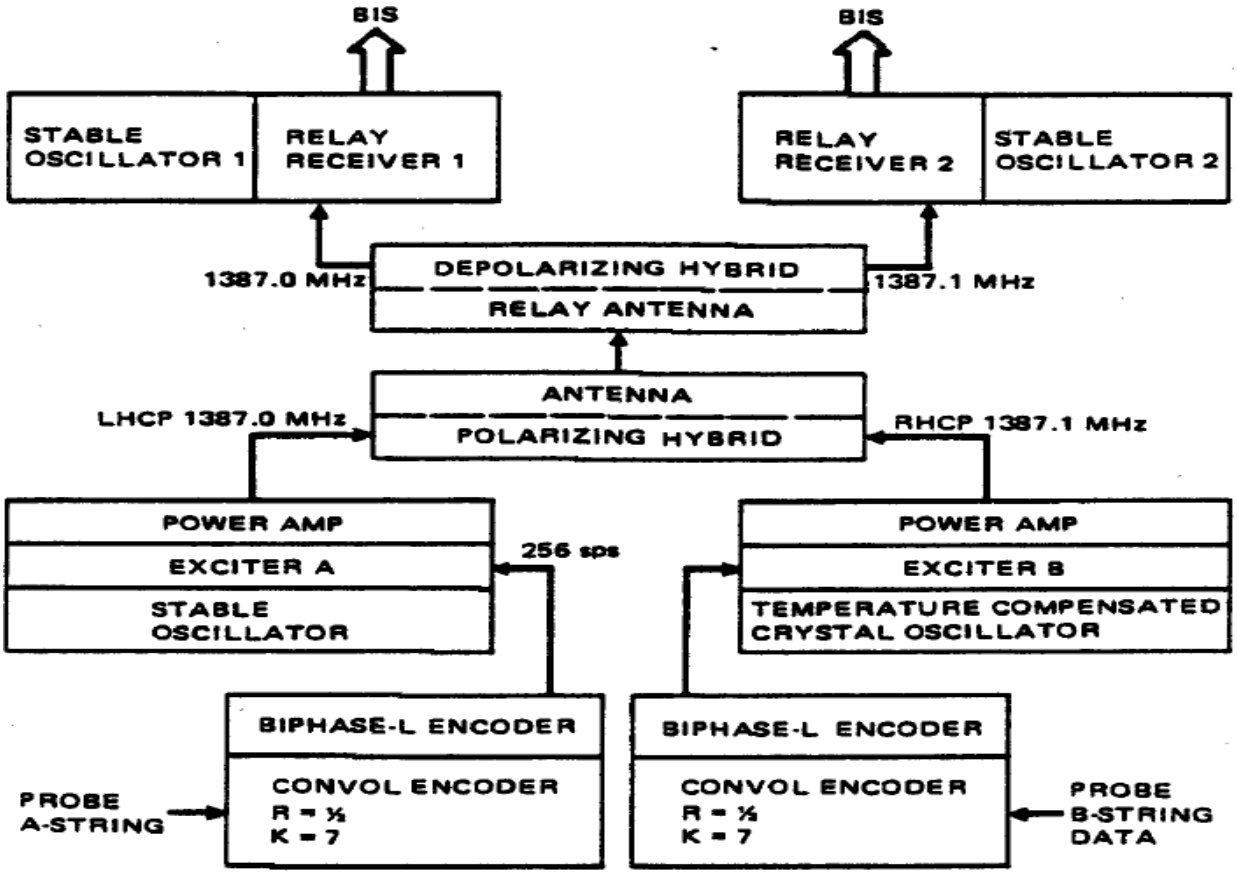

Fig. 7-1. Probe/RRH communications block diagram.

Each power amplifier in the probe output an RF level of 23 W to the antenna, one carrying A-string data and the other B-string data. The carriers first passed through a polarizing hybrid that made the 1387 downlink LCP and the 1387.1 MHz downlink RCP. Each active unit (encoder, exciter, power amplifier) was enclosed in a sealed pressurized container, designed to survive to a pressure of 20 bars.

The probe antenna was a crossed dipole cup. For both frequencies, the antenna gain was 10 dBi, with a beamwidth of 56 deg between the half-power points. The antenna was fixed to the aft end of the probe, with its boresight intended to remain generally aligned to the local vertical throughout descent.

After leaving the probe antenna, the RF signals traversed a portion of the Jovian atmosphere, suffering absorption by ammonia and by clouds that were anticipated to exist in the region between 2.5 to 6.3 bars pressure. The signals also suffered fading due to scintillation in Jupiter's ionosphere. Predicted link performance was based on a relay communications range between 214,000 km at entry to 229,000 km an hour later.

At the orbiter the RRA, a 1.1-m parabolic dish, received the carriers. The RRA gain was 21.0 dB peak, with a 25-deg beamwidth between the half-power points. The RRA also received background noise from Jupiter's disk and from synchrotron activity in the Jovian magnetosphere. The two carriers were separated by a depolarizing hybrid that output them to each of the two RRH receivers. Each receiver had a USO[3] of essentially the same design as the one in the probe.

Each receiver acquired, tracked, and demodulated one of the channels. When in the phase-locked mode, the receiver provided estimates of the (signal + noise) amplitude and the noise amplitude for downlink in the probe data from the orbiter. The receiver also provided the numerically controlled oscillator (NCO) control word for use in estimating the signal frequency and changes in signal frequency. More receiver detail, including a description of software algorithms, is in [30].

The detected symbols were output from a 3-bit soft-quantizer, each symbol thus providing a sign and a relative level. The detected symbols were not further decoded, but rather stored onboard the orbiter for later transmission to the Earth on the S-band downlink.

The orbiter targeting, articulation of the relay radio antenna (RRA), and near-JOI sequence of events were required to allow acquisition of at least 60 minutes of data from the probe, with up to 75 minutes if other constraints allowed. The orbiter was to provide the RRA with a minimum unobstructed field of view of 12 deg half cone angle, from the edge of the antenna, for all required pointing directions.

The orbiter's sequence of activities was to include returning at least the first 39 minutes of the relay data in real time. This is based on an assumed knowledge accuracy of 75 s, at 99% confidence, for probe entry time. The Jupiter arrival date and geometry were chosen to avoid solar conjunction interference with the return of the initial probe data and to avoid having the relay signal pass through Jupiter's rings.

Relay link performance at 10 bars atmospheric pressure was based on achieving a BER of less than 1/1000, at 128 bps. The link was required to have positive margin relative to 99% adverse environmental tolerances plus the root sum square of the 99% system performance tolerances. Probe link lockup was to occur about 70 s after parachute (chute) deployment at about 0.8 bars atmospheric pressure.

7.3 Summary of Achieved Relay-Link Performance

The initial downlink from the orbiter memory readouts (MRO) showed both A-string and B-string downlinks had locked up. The quality bits attached to the probe symbols were all "high," indicating the communications link was solid. Orbiter telemetry verified the RRA successfully went through its four commanded repositionings to maintain the communications link. The first (pre-conjunction) MRO provided an overall look at the probe mission. The B-string data lasted to entry + 51.2 minutes (approximately 13 bars pressure in the worst-case model, and the A-string to entry + 61.4 minutes.[4] A "coast timer" had begun counting down at

[3] These USOs are distinct from the USO associated with the orbiter's S-band downlink in the one-way mode.

[4] See [29], from which these times came. Times of 48.3 minutes (B string) and 58.5 minutes (A string) are also given, relative to a reference of major/minor frame zero (MF 0). Entry was 166 s prior to MF 0.

separation of the probe from the orbiter. This timed out accurately, resulting in successful acquisition of pre-entry data. The MRO also showed all probe science instrument were working and returning data.

The signal level at the RRH was more than sufficient to maintain lock for the entire mission. The reported signal level was an average of 1.5 to 2 dB lower than predicted. Possible causes for the discrepancy were analyzed, including RRA mispointing, changes in hardware performance since launch, and calibration errors (less likely). The carrier to noise ratio (P_c/N_0) was in the range of +35 to +40 dBm for both A-string and B-string from entry to entry + 50 minutes. A-string fell to 28 dBm before recovering to 31 dBm just before it went out of lock. During the major part of descent, the Probe link P_c/N_0 was well above the threshold of ~26 dB, and no bit errors occurred.

The MRO data from both RRH strings showed that loss-of-lock was preceded by a sudden drop in the transmitted power. The temperature of the probe communications equipment was about 115 C, higher than expected and well above the 60 C qualification temperature.

Section 8

Lessons Learned

Don’t fly a complex system that has single points of failure if simpler systems can provide sufficient performance.

As expressed in JPL’s principles for flight systems [32]:

1. Designs shall employ a “keep-it-simple” philosophy (straightforward designs) to reduce risk/cost, to enable easy implementation, design verification and flight operational usage.
2. Use of “complex” design implementations shall be avoided. Added complexity shall be justified to be essential to meet mission requirements or constraints.

The deployable Galileo HGA was 4.8 m in diameter, as compared with the 3.7-m solid Voyager HGA. Disregarding all factors other than planned communication capability, this is a difference of about 2 dB. The GLL HGA was based on, but not identical to, the TDRS deployable antenna.

Back up critical spacecraft functions.

The cost of including backup (redundant) hardware is spacecraft mass and perhaps complexity. The risk of not including it is the loss of the mission. There have been two situations involving telecom functions that made us glad to have a backup.

3. Receiver-A developed the “wandering VCO volts” anomaly, which eventually cleared. A working receiver is essential to continuing a mission, and Galileo continues with Receiver-B in reserve.
4. The USO frequency, because it is so stable, has been observed to be affected by the radiation environment near Jupiter. In 2001–2002 there may have also been a transient condition in which abrupt frequency shifts occurred, severe enough to cause loss of downlink lock. An onboard RF frequency source, while possibly not essential to mission continuation, is certainly reassuring. An aux osc in each S-EXC, provides a separate means to generate a one-way downlink in the absence of the single USO.

Model and handle telecom link margin wisely.

The S-band mission has required Galileo to make use of link margin aggressively though not recklessly. Repeated inflight measurements of SNR and SNT resulted in changes to the modeled LGA-1 antenna pattern and updates to the DSN interface documents [9, 10]. This work also established that spacecraft and station performance was stable and accurately modeled in the prediction tool. The project established a margin policy for data rate sequencing. The policy is that the transition point for switching up or down in data rate is at a time when the predicted mean P_t/N_0 is 0.5 dB higher than the threshold of the higher data rate. This 0.5-dB margin is much lower than on the typical deep space mission. It was established as an optimum level that results in the loss of only occasional telemetry frames but that prudently maximizes the sequenced bits-to-ground data volume for every pass.

The S-band mission performance improvement techniques are reusable.

Development of the onboard data compression and advanced error-correcting coding while Galileo was in flight, and the concurrent development of intercontinental arraying of ground stations and the feedback concatenated decoder were necessary to save the mission. The Galileo mission very costly in terms of DSN tracking time required.

A lesson learned from the success of this development has been applied to reduce tracking time of deep-space missions after Galileo. As expressed in [32]:

> To [accommodate] limited DSN tracking pass capability, the information system design shall consider significant use of data editing, data compression, and improved data encoding techniques to meet downlink telemetry data requirements.

Epilogue

Remote sensing.

A sad milestone was reached by Galileo on March 30, 2002, when the last bit of remote sensing data "hit the ground" following a long and impressive history of discovery. The Ultraviolet Spectrometer, Solid State Imaging camera, Photopolarimeter/Radiometer, and Near Infrared Mapping Spectrometer have answered some of the fundamental questions about Jupiter's atmosphere and satellites as well as expanding our knowledge of asteroids and cometary impacts into gaseous planets. Through their "eyes" we have observed the moon orbiting Earth and Dactyl orbiting Ida; giant geyser-like plumes and fire fountains erupting on Io; salty ices and broken "ice raft" blocks on the surface of fractured Europa; white ovals and brown barges appear and merge in the clouds of Jupiter; huge strike-slip offsets along fractures on Ganymede; unexpected heat flow patterns on Io; and sublimation erosion of Callisto. This is just a sampling of the legacy of the Galileo remote sensing experiments.

Eilene Theilig
Galileo Project Manager

Radio science.

Unique among the orbiter and probe investigations, radio science has used the onboard radios and the Deep Space Network as its instrumentation. Radio science investigations helped to resolve long-standing questions about Jupiter's ionosphere, and made possible multiple measurements of the ionospheres and plasma environments of Io, Europa, Ganymede and Callisto, and the internal structure of the Galilean satellites. The lengthy mission with its periodic solar oppositions and conjunctions has also given radio science an opportunity to study the solar corona over nearly the whole period of an 11-year solar cycle.

The propagation experiments revealed the high degree of variability of Jupiter's ionosphere, asymmetrical ionospheres at Europa and Io, a well developed classical ionosphere at Callisto, and no observable ionosphere at Ganymede. The gravity measurements revealed the possible internal structures of the Galilean satellites: Io has no icy crust and is virtually all rock with an iron/iron sulfide core; Europa has a relatively thin ice (and maybe liquid) shell over its differentiated core; Ganymede has a much thicker icy shell; and Callisto seems to be quite undifferentiated internally.

A historic Radio Science occasion during Galileo was the first use of the DSN radio science system remote operations, with the instrument controlled from JPL to conduct these experiments. Galileo has also provided an environment for developing efficient radio science multi-mission tools such as data acquisition, transfer, delivery, validation, and analysis that have been a great benefit for later missions.

Aseel Anabtawi
Galileo Radio Science Team

References

[1] *Galileo Orbiter Telecommunications Design Control Document*, Galileo Project Document 625-257, JPL internal document, March 1983.

[2] *Galileo Orbiter Functional Requirements*, Galileo Project Documents 625-205:

Equipment List and Mass Allocations, module GLL-3-230

Power Profiles and Allocations, module GLL-3-250

Galileo Telecom Requirements, module GLL-3-300

Modulation Demodulation Subsystem Requirements, module GLL-4-2003

Radio Frequency Subsystem Requirements, module GLL-4-2004

S/X Band Antenna Subsystem Requirements, module GLL-4-2017.

[3] Galileo project website, http://www.jpl.nasa.gov/galileo/

[4] D. J. Mudgway, *Uplink-Downlink: a History of the Deep Space Network 1957–1997*, National Aeronautics and Space Administration, Washington, D.C., 2001.

[5] JPL external website (includes information on Galileo as well as other projects), http://www.jpl.nasa.gov/missions/current/galileo.html

[6] P. E. Beyer, B. G. Yetter, R. G. Torres, and D. J. Mudgway, "Deep Space Network Support for the Galileo Mission to Jupiter: Jupiter Orbital Operations from Post-Jupiter Orbit Insertion Through the End of the Prime Mission," *TDA Progress Report 42-133*, May 15, 1998, http://tmo.jpl.nasa.gov/tmo/progress_report/42-133/133A.pdf

[7] W. Mayo and F. H. Taylor, "Orbiter Telecom Subsystem and Orbiter Link Performance," Galileo project memo, December 17, 1997, http://sso:82/glldocs/OET_finalRPT/OETFinalRpt.shtml

[8] *Network Operations Plan for Galileo Project*, Vol. II, Rev. D, *Operations Manual*, DSN 870-7, issue date June 26, 1996, JPL D-1997.

[9] *DSMS Telecommunications Link Design Handbook*[1], JPL 810-005, Rev. E, http://eis.jpl.nasa.gov/deepspace/dsndocs/810-005/

[10] R. Sniffin, *Deep Space Network/Flight Project Telecommunications Interface Design Document*, JPL 810-5, Rev. D, http://block/810-5/810-5.html

[11] R. Ludwig and F. H. Taylor, "Voyager Telecommunications," *Design and Performance Analysis Series*, Article 4, http://descanso.jpl.nasa.gov/index_ext.html

[12] P. E. Beyer, R. C. O'Connor, and D. J. Mudgway, "Galileo Early Cruise, Including Venus, First Earth, and Gaspra Encounters," *TDA Progress Report 42-109*, May 15, 1992, http://tmo.jpl.nasa.gov/tmo/progress_report/42-109/109T.PDF

[13] *The Evolution of Technology in the Deep Space Network: Advanced Systems Program and the Galileo Mission to Jupiter*, http://deepspace.jpl.nasa.gov/technology/95_20/gll_case_study.html

[1] There are two versions of the tracking-station-interface document, with Rev. D [10] applicable through most of the Galileo mission. Rev. D of 810-5 is dated February 15, 1975 (with later individual release dates of many individual modules). The document was superseded and renamed 810-005 (Rev. E) [9], January 15, 2001.

[14] K.-M. Cheung, K. Tong, and T. Chauvin, "Enhancing the Galileo Data Return Using Advanced Source and Channel Coding," *Proceedings of the NASA Technology 2004 Conference*, Washington D.C., September 1994.

[15] S. Dolinar and M. Belongie, "Enhanced Decoding for the Galileo Low-Gain Antenna Mission: Viterbi Redecoding with Four Decoding Stages," *TDA Progress Report 42-121*, May 15, 1995, http://tmo.jpl.nasa.gov/tmo/progress_report/42-121/121Q.pdf

[16] K.-M. Cheung and S. J. Dolinar, Jr., "Performance of Galileo's Concatenated Codes With Non-ideal Interleaving," *TDA Progress Report 42-95*, July-September 1988, pp. 148–152, November 15, 1988.

[17] J. H. Yuen, editor, *Deep Space Telecommunications Systems Engineering*, Plenum Press, 1983.

[18] J. H. Yuen, "A Practical Statistical Model for Telecommunications Performance Uncertainty," JPL technical memorandum 33-732, June 15, 1975.

[19] R. H. Tung, "User's Guide, Telecom Forecaster Predictor/Unified Telecom Predictor (TFP/UTP),V2.1," *DSMS No. 887-000036*, February 21, 2002.

[20] K. K. Tong and R. H. Tung, *A Multimission Deep-Space Telecommunications Analysis Tool: The Telecom Forecaster Predictor*, http://tmo.jpl.nasa.gov/tmo/progress_report/42-140/title.htm

[21] http://science.ksc.nasa.gov/shuttle/missions/sts-34/mission-sts-34.html (especially the Press Kit). Details are in http://sdtss10.fltops.jpl.nasa.gov/archive/archive.html (internal to JPL).

[22] Galileo mission phases, http://www.jpl.nasa.gov/galileo/mission/mission.html

[23] D. L. Gray, "Delta VLBI Data Performance in the Galileo Spacecraft Earth Flyby of December 1990," *TDA Progress Report 42-106*, April-June 1991, pp. 335–352, August 15, 1991, http://tmo.jpl.nasa.gov/tmo/progress_report/42-106/106X.PDF

[24] W. J. O'Neil, "Project Galileo Mission Status," IAF-91-468, *42nd Congress of the International Astronautical Federation*, Montreal, Canada, October 5–11, 1991.

[25] http://quest.arc.nasa.gov/galileo/Galileo-QA/Antennae/Problem_opening_antenna.1 (accessed from T. V. Johnson, "The Galileo Mission to Jupiter and Its Moons," *Scientific American*, February 2000, http://www.sciam.com/2000/0200issue/0200johnson.html)

[26] W. J. O'Neil, N. E. Ausman Jr., Torrence V. Johnson, and M. R. Landano, "Galileo Completing VEEGA—a Mid-Term Report," IAF-92-0560, *43rd Congress of the International Astronautical Federation*, Washington, D.C., August 28–September 5, 1992.

[27] W. J. O'Neil, N. E. Ausman Jr., T. V. Johnson, M. R. Landano, and J. C. Marr, "Performing the Galileo Jupiter Mission with the Low-Gain Antenna (LGA) and an Enroute Progress Report," IAF-93.Q.5.411, *44th Congress of the International Astronautical Federation*, Graz, Austria, October 16–22, 1993.

[28] E. Theilig and D. Bindschadler, *Galileo Friday Report*, weekly e-mail status reports to JPL and NASA Headquarters (JPL internal document).

[29] *Galileo Probe Mission Operations Final Report*, Hughes Space and Communications Company, Contract NAS2-10000, September 1996.

[30] *Galileo Probe Operations Manual, Vol. 1, Probe/RRH System Description*, Hughes Aircraft Co., E1812, SCG 850509R, undated but released prior to launch.

[31] L. E. Bright, *Galileo Probe-Orbiter Relay Link Integration Report*, Rev. A, 1625-145, January 16, 1984.

[32] M. R. Landano, “Design, Verification/Validation and Operations Principles for Flight Systems,” JPL D-17868, Rev. A, (JPL internal document) November 15, 2000.

Additional Resources

- Galileo artwork, http://www.jpl.nasa.gov/galileo/images/artwork.html
- GLL-625-10 (GEM Mission Plan) and GLL-625-11 (GMM Mission Plan) in http://sso:82/glldocs/OET_finalRPT/OETFinalRpt.shtml (JPL internal document).

Abbreviations and Acronyms

ACE	call sign (not an acronym) of real-time mission controller
ACIS	antenna control and interface subsystem
AGC	automatic gain control (received carrier power)
AU	astronomical unit (~1.496×10^8 km)
aux osc	auxiliary oscillator
AWGN	additive white Gaussian noise
BER	bit-error rate
BLF	best-lock frequency
bps	bits per second
BTD	buffered telemetry demodulator
BVR	block 5 receiver
BW	bandwidth
CDS	command data subsystem
CDU	command detector unit
CLBW	carrier-loop bandwidth
clk	clock
CMA	command modulator assembly
CMD	command
CME	coronal-mass ejection
CNR	carrier-to-noise ratio
CPA	command processor assembly
CPLR	coupler
CSIRO	Commonwealth Scientific and Industrial Research Organization (Australia)
dB	decibel
dBi	decibel with respect to isotropic gain
dBm	decibel referenced to milliwatts
DCO	digital control oscillator
DCT	design control table
DCT	discrete cosine transform
deg	degree
DESCANSO	Deep Space Communications and Navigation Systems Center of Excellence
DGT	DSCC Galileo telemetry
DOFF	degrees off boresight
DOR	differential one-way ranging
DOY	day of year
DPLXR	diplexer
DRCF	data rate capability file
DSCC	Deep Space Communications Complex
DSN	Deep Space Network
DSS	Deep Space Station
E_b/N_0	bit-energy-to-noise spectral density ratio
EIRP	effective isotropically radiated power
E_s/N_0	symbol-energy-to-noise spectral density ratio
EXC	exciter
FCD	feedback concatenated decoder

FSC	full-spectrum combiner
FSR	full-spectrum recorder
FSS	frame-synchronizer subsystem
GEM	Galileo Europa Mission
GLL	Galileo
GMM	Galileo Millennium Mission
GSOC	German Spaceflight Operations Center
HEMT	high electron mobility transistor
HGA	high-gain antenna
Hz	hertz
IF	intermediate frequency
IND	Interplanetary Network Directorate
IUS	Inertial Upper Stage
JOI	Jupiter orbit insertion
JPL	Jet Propulsion Laboratory
LCP	left circular polarization
LGA	low-gain antenna
LH2	cryogenic liquid hydrogen (fuel)
LNA	low-noise amplifier
Lox	cryogenic liquid oxygen (oxidizer)
MCD	maximum likelihood convolutional decoder
MDS	modulation demodulation subsystem
Mod	modulation
MRO	memory readout
MZPOINT	–Z axis pointing
NASA	National Aeronautics and Space Administration
NCO	numerically controlled oscillator
OWLT	one-way light time
P_c/N_0	carrier-power-to-noise spectral density ratio
PNT	pointing
P_r/N_0	ranging-power-to-noise spectral density ratio
PRA	planetary radio astronomy
P_t/N_0	total-power-to-noise spectral density ratio
RCP	right circular polarization
RCVR	receiver
RF	radio frequency
RFS	radio frequency subsystem
RFSTLC	RFS tracking-loop capacitor
Rj	Jupiter radius (71,992 km)
RRA	relay radio antenna
RRH	relay radio hardware
RS	Reed-Solomon
RTG	radioisotope thermoelectric generator
RTLT	round-trip light time
SEC	Sun-Earth-craft angle
SEP	Sun-Earth-probe angle; same as SEC angle
SPD	S-band polarization diversity
SRA	sequential ranging assembly

SRM	solid rocket motor
SSI	solid-state imaging
STS	Space Transportation System (shuttle)
SXA	S- and X-band antenna
sync	synchronization
TCA	telemetry channel assembly
TDM	time division multiplex
TDRS	Tracking Data Relay Satellite
TDRSS	Tracking Data Relay Satellite System
TFP	telecom forecaster predictor
TFREQ	transmit frequency message
TLM	telemetry
TLMGEN	telemetry generator
TMOD	Telecommunications and Mission Operations Directorate (now IND)
TMU	telemetry modulation unit
TW	truth window
TWNC	two-way non-coherent
TWTA	traveling-wave-tube amplifier
U/L ACQ	uplink acquisition
USO	ultrastable oscillator
UTC	Universal Time Coordinated
VCO	voltage-controlled oscillator
VEEGA	Venus-Earth-Earth gravity assist
VLA	Very Large Array (Socorro, NM)
XB	X-band
XSDC	X- to S-band downconverter